

# Fisher-Rao distance and pullback SPD cone distances between multivariate normal distributions\*

Frank Nielsen 

Sony Computer Science Laboratories Inc.  
Tokyo, Japan

## Abstract

Data sets consisting of multivariate normal distributions abound in many scientific areas like diffusion tensor imaging, structure tensor computer vision, radar signal processing, machine learning, etc. In order to process those normal data sets for downstream tasks like filtering, classification, or clustering, one needs to define proper notions of dissimilarities between normals and smooth paths linking them. The Fisher-Rao distance defined as the Riemannian geodesic distance induced by the Fisher information metric is such a principled metric distance which however is not known in closed-form excepts for a few particular cases including the univariate and same-mean/same-covariance cases. In this work, we first report a fast and robust method to approximate the Fisher-Rao distance between multivariate normal distributions with a guaranteed  $1 + \epsilon$  factor for any  $\epsilon > 0$ . Second, we introduce a class of distances based on diffeomorphic embeddings of the normal manifold into a submanifold of the higher-dimensional symmetric positive-definite cone corresponding to the manifold of centered normal distributions. We show that the projective Hilbert distance on the cone yields a metric distance on the embedded normal submanifold, and we pullback that cone distance with its associated straight line Hilbert cone geodesics to obtain a distance and smooth paths between normal distributions. Compared to the Fisher-Rao distance approximation, the pullback Hilbert cone distance is computationally light since it requires to compute only the extreme minimal and maximal eigenvalues of matrices. Finally, we show how to use those distances and paths in clustering tasks.

## 1 Introduction

Data sets of multivariate normal distributions (MVNs) are increasing frequent in many scientific areas like medical imaging (diffusion tensor imaging [40]), computer vision (image segmentation [22] or structure tensor imaging [63]), signal processing (covariance matrices [11] in radar or brain computer interfaces [10]), and machine learning (Gaussian mixtures or kernel density estimators [28]). These data sets can be viewed as (weighted) point sets on a Gaussian manifold and Riemannian and information-geometric structures [67, 77] on that manifold allows one to define geodesics and distances or divergences which allows on to build algorithms like filtering, classification, clustering or optimization techniques [74, 1, 43]. For example, we may simplify a Gaussian mixture model [28, 37, 79] (GMM) with  $n$  components by viewing the mixture as a weighted point set and simplify the mixture by clustering the point set into  $k$  clusters using  $k$ -means or  $k$ -medioids [28] (as known as discrete  $k$ -means). We may also consider  $n$  GMMs with potentially different components and build a codebook of all mixture components to quantize and compress the representation of these GMMs. In this work, we consider two kinds of metric distances and metric geodesics: The Fisher-Rao distance [69] and a new distance obtained by pulling back the Hilbert cone projective distance on an embedding of the Gaussian manifold into the higher-dimensional symmetric positive-definite matrix cone [20].

---

\*A preliminary version of this work appeared as “Fisher-Rao and pullback Hilbert cone distances on the multivariate Gaussian manifold with applications to simplification and quantization of mixtures,” at the 2nd Annual Topology, Algebra, and Geometry in Machine Learning Workshop (TAG-ML) of ICML’23.

The paper is organized as follows: In Section 2, we recall the Fisher-Rao geodesic distance and mention its lack of general closed-form formula on the Gaussian manifold. We then build on a recent breakthrough which studied the MVN Fisher-Rao geodesics [49] (§2.2) to design an approximation method which upper bounds the true Fisher-Rao distance with guaranteed  $(1 + \epsilon)$  precision for any  $\epsilon > 0$  (Theorem 2.2 in §2.3). We present applications to simplification and quantization of GMMs in Section 3 using fast clustering methods relying on nearest neighbor query data structures [76] and smallest enclosing balls in metric spaces. In Section 4, we introduce the novel pullback Hilbert cone distance which is fast to compute and enjoys simple expression of geodesics.

## 2 Fisher-Rao geodesics and distances

A normal distribution  $N(\mu, \Sigma)$  has probability density function (pdf)  $p_{\mu, \Sigma}(x)$  defined on the full support  $\mathbb{R}^d$  given by:

$$p_{\mu, \Sigma}(x) = \frac{(2\pi)^{-\frac{d}{2}}}{\sqrt{\det(\Sigma)}} \exp\left(-\frac{(x - \mu)^\top \Sigma^{-1}(x - \mu)}{2}\right).$$

Consider the statistical model consisting of all  $d$ -variate normal distributions:

$$\mathcal{N}(d) = \{N(\lambda) : \lambda = (\mu, \Sigma) \in \Lambda(d) = \mathbb{R}^d \times \text{Sym}_+(d, \mathbb{R})\},$$

where  $\text{Sym}_+(d, \mathbb{R})$  denote the set of  $d \times d$  positive-definite matrices. The dimension of  $\mathcal{N}(d)$  is  $m = \dim(\Lambda(d)) = d + \frac{d(d+1)}{2} = \frac{d(d+3)}{2}$ . When the dimension is clear from context, we omit to specify the dimension and write  $\mathcal{N}$  for short.

Let  $l_\lambda(x) = \log p_\lambda(x)$  denote the log-likelihood function. The MVN model is both identifiable (bijection between  $\lambda$  and  $p_\lambda$ ) and regular [19, 5], i.e., the Fisher information matrix  $I(\theta) = -E_\theta[\nabla^2 l_\theta(x)]$  is positive-definite and defines a Riemannian metric  $g_{\text{Fisher}}$  called the Fisher information metric. The Riemannian manifold  $(\mathcal{N}, g_{\text{Fisher}})$  is called the Fisher-Rao Gaussian manifold with squared infinitesimal length element [67]  $ds_{\text{Fisher}}^2$  at  $(\mu, \Sigma)$  given by:

$$ds_{\text{Fisher}}^2 = d\mu^\top \Sigma^{-1} d\mu + \frac{1}{2} \text{tr}\left((\Sigma^{-1} d\Sigma)^2\right),$$

where  $d\mu \in \mathbb{R}^d$  and  $d\Sigma \in \text{Sym}(d, \mathbb{R})$  (vector space of symmetric  $d \times d$  matrices).

The Fisher-Rao length of a smooth curve  $c(t)$  with  $t \in [a, b]$  is defined by integrating the infinitesimal Fisher-Rao length element along the curve:  $\text{Len}(c) = \int_a^b ds_{\text{Fisher}}(c(t)) dt$ , and the Fisher-Rao distance [44, 64] between  $N_0 = N(\mu_0, \Sigma_0)$  and  $N_1 = N(\mu_1, \Sigma_1)$  is the geodesic distance on  $(\mathcal{N}, g_{\text{Fisher}})$ , i.e., the length of the Riemannian geodesic  $\gamma_{\text{FR}}^{\mathcal{N}}(N_0, N_1; t)$ :

$$\rho_{\text{FR}}(N_0, N_1) = \int_0^1 ds_{\text{Fisher}}(\gamma_{\text{FR}}^{\mathcal{N}}(N_0, N_1; t)) dt. \quad (1)$$

In Riemannian geometry [36], geodesics with boundary conditions  $N_0 = \gamma_{\text{FR}}^{\mathcal{N}}(N_0, N_1; 0)$  and  $N_1 = \gamma_{\text{FR}}^{\mathcal{N}}(N_0, N_1; 1)$  are length minimizing curves among all curves  $c(t)$  satisfying  $c(0) = N(\mu_0, \Sigma_0)$  and  $c(1) = N(\mu_1, \Sigma_1)$ :

$$\rho_{\text{FR}}(N_0, N_1) = \inf_{\substack{c(t) \\ c(0)=p_{\mu_0, \Sigma_0} \\ c(1)=p_{\mu_1, \Sigma_1}}} \{\text{Len}(c)\}.$$

Riemannian geodesics are parameterized by (normalized) arc length  $t$  which ensures that

$$\rho(\gamma_\rho(P_0, P_1; s), \gamma_\rho(P_0, P_1; t)) = |s - t| \rho(P_0, P_1). \quad (2)$$

More generally, geodesics in differential geometry [19] are auto-parallel curves with respect to an affine connection  $\nabla$ :  $\nabla_{\dot{\gamma}}\dot{\gamma} = 0$ , where  $\dot{\cdot} = \frac{d}{dt}$  and  $\nabla_X Y$  is the covariant derivative induced by the connection. In Riemannian geometry, the default connection is the unique *Levi-Civita metric connection* [36]  $\nabla^g$  induced by the metric  $g$ .

In general, the Fisher-Rao distance between MVNs is not known in closed-form [62, 56]. However, there are two main cases where closed-form formula are known:

- The case  $d = 1$ : The Fisher-Rao distance between univariate normal distributions [78]  $N_0 = N(\mu_0, \sigma_0^2)$  and  $N_1 = N(\mu_1, \sigma_1^2)$  is

$$\rho_{\mathcal{N}}(N_0, N_1) = \sqrt{2} \log \left( \frac{1 + \Delta(\mu_0, \sigma_0; \mu_1, \sigma_1)}{1 - \Delta(\mu_0, \sigma_0; \mu_1, \sigma_1)} \right), \quad (3)$$

where for  $(a, b, c, d) \in \mathbb{R}^4 \setminus \{0\}$ ,

$$\Delta(a, b; c, d) = \sqrt{\frac{(c-a)^2 + 2(d-b)^2}{(c-a)^2 + 2(d+b)^2}} \quad (4)$$

is a Möbius distance [17].

- The case where MVNs  $N_0$  and  $N_1$  share the same mean [46, 67], i.e., they belong to some submanifold  $\mathcal{N}_\mu = \{N(\mu, \Sigma) : \Sigma \in \text{Sym}_+(d, \mathbb{R})\}$ . When  $\mu = 0$ , we let  $\mathcal{P}(d) = \mathcal{N}_0(d)$ . We have:

$$\rho_{\mathcal{N}_\mu}(N_0, N_1) = \sqrt{\frac{1}{2} \sum_{i=1}^d \log^2 \lambda_i(\Sigma_0^{-\frac{1}{2}} \Sigma_1 \Sigma_0^{-\frac{1}{2}})}, \quad (5)$$

where  $\lambda_i(M)$  denotes the  $i$ -th largest eigenvalue of matrix  $M$ . Observe that matrix  $\Sigma_0^{-1} \Sigma_1$  may not be symmetric but  $\Sigma_0^{-\frac{1}{2}} \Sigma_1 \Sigma_0^{-\frac{1}{2}}$  is always SPD and  $\lambda_i(\Sigma_0^{-1} \Sigma_1) = \lambda_i(\Sigma_0^{-\frac{1}{2}} \Sigma_1 \Sigma_0^{-\frac{1}{2}})$ . The submanifolds  $\mathcal{N}_\mu$  are totally geodesic in  $\mathcal{N}$ , and the Fisher-Rao geodesics are known in closed form:  $\gamma_{\text{FR}}^{\mathcal{N}}(N_0, N_1; t) = N(\mu, \Sigma_t)$  with

$$\Sigma_t = \Sigma_0^{\frac{1}{2}} (\Sigma_0^{-\frac{1}{2}} \Sigma_1 \Sigma_0^{-\frac{1}{2}})^t \Sigma_0^{\frac{1}{2}}. \quad (6)$$

The geodesic  $\gamma(\Sigma_0, \Sigma_1; t) = \Sigma_t$  (with  $t \in [0, 1]$ ) midpoint is thus

$$\gamma(\Sigma_0, \Sigma_1; \frac{1}{2}) = \Sigma_{\frac{1}{2}} = \Sigma_0^{\frac{1}{2}} (\Sigma_0^{-\frac{1}{2}} \Sigma_1 \Sigma_0^{-\frac{1}{2}})^{\frac{1}{2}} \Sigma_0^{\frac{1}{2}}.$$

See also Appendix C.

Notice that all submanifolds  $\mathcal{N}_\mu$  are non-positive curvature manifolds (NPC) [16, 25], i.e. sectional curvatures are non-positive. However,  $\mathcal{N}(d)$  is not a NPC manifold when  $d > 1$  since some sectional curvatures can be positive [67]. NPC property is important for designing optimization algorithms on manifolds with guaranteed convergence [25]. In a NPC manifold  $(M, g)$ , we can write the Riemannian distance using the Riemannian logarithm map  $\text{Log}_p : M \rightarrow T_p M$ :  $\rho_g(p_1, p_2) = \|\text{Log}_{p_1}(p_2)\|_{p_1}$ , where  $\|v\|_p = \sqrt{g_p(v, v)}$ . On the NPC SPD cone  $\text{Sym}_+(d, \mathbb{R})$  equipped with the trace metric [54, 29]

$$g_P^{\text{trace}}(P_1, P_2) := \text{tr}(P^{-1} P_1 P^{-1} P_2),$$

the length element at  $P$  is  $ds_P = \|P^{-\frac{1}{2}} dP P^{-\frac{1}{2}}\|_F$ , and the Riemannian logarithm map is expressed using the matrix logarithm  $\text{Log}$ , and we have

$$\rho_{g_{\text{trace}}}(P_1, P_2) = \|\text{Log}_{P_1}(P_2)\|_{P_1} = \|\text{Log}(P_1^{-1} P_2)\|_F,$$

where  $\|X\|_F = \sqrt{\langle X, X \rangle_F} = \sqrt{\sum_{i,j} X_{ij}^2}$  is the Frobenius norm induced by the Frobenius inner product:  $\langle A, B \rangle_F = \text{tr}(A^\top B)$  (Hilbert-Schmidt inner product). The Frobenius norm can be calculated in quadratic time as  $\|M\|_F = \sqrt{\sum_{i,j=1}^d m_{ij}^2}$  for a  $d \times d$  matrix  $M = [m_{ij}]$ , and is equivalent to the  $\ell_2$  norm on the vectorization of  $M$ :  $\|M\|_F = \|\text{vec}(M)\|_2$ , where  $\text{vec}(M) = [m_{11}, \dots, m_{1d}, \dots, m_{d1}, \dots, m_{dd}]^\top \in \mathbb{R}^{d^2}$ . The SPD cone is also a Bruhat-Tits space [52].

Historically, the SPD Riemannian trace metric distance was studied by Siegel [66] in the wider context of the complex manifold of symmetric complex square matrices with positive-definite imaginary part: The so-called Siegel upper half space [33] which generalizes the Poincaré upper plane. It was shown recently that the Siegel upper half space is NPC [18]. Another popular distance in machine learning in the Wasserstein distance for which the underlying geometry on the Gaussian space was studied in [71].

## 2.1 Invariance under action of the positive affine group

The length element  $ds_{\text{Fisher}}$  is invariant under the action of the positive affine group [31, 32]

$$\text{Aff}_+(d, \mathbb{R}) := \{(a, A) : a \in \mathbb{R}^d, A \in \text{GL}_+(d, \mathbb{R})\},$$

where  $\text{GL}_+(d, \mathbb{R})$  denotes the group of  $d \times d$  matrices with positive determinant. The group identity element of  $\text{Aff}_+(d, \mathbb{R})$  is  $e = (0, I)$  and the group operation is  $(a_1, A_1) \cdot (a_2, A_2) = (a_1 + A_1 a_2, A_1 A_2)$  with inverse operation  $(a, A)^{-1} = (-A^{-1}a, A^{-1})$ . The positive affine group may be handled as a matrix group by mapping elements  $(a, A)$  to  $(d+1) \times (d+1)$  matrices  $M_{(a,A)} := \begin{bmatrix} A & a \\ 0 & 1 \end{bmatrix}$ . Then the matrix group operation is the matrix multiplication and inverse operation is given by the matrix inverse. Let us consider the following group action (denoted by the dot  $\cdot$ ) of the positive affine group on the Gaussian manifold  $\mathcal{N}$ :

$$(a, A) \cdot N(\mu, \Sigma) = N(a + A\mu, A\Sigma A^\top).$$

This action corresponds to the affine transformation of random variables:  $Y = a + AX \sim N(a + A\mu, A\Sigma A^\top)$  where  $X \sim N(\mu, \Sigma)$ . The statistical model  $\mathcal{N}$  can thus be interpreted as a group with identity element the standard MVN  $N_{\text{std}} = N(0, I)$ :  $\mathcal{N}(d) = \{(a, A) \cdot N_{\text{std}} : (a, A) \in \text{Aff}_+(d)\}$ . We get a Lie group differential structure on  $\mathcal{N}$  [51] which moreover extends to a statistical Lie group structure in information geometry [34].

It can be checked that the Fisher-Rao length element is invariant under the action of  $\text{Aff}_+(d, \mathbb{R})$  and therefore the Fisher-Rao distance is also invariant:  $\rho_{\text{FR}}((a, A) \cdot N_0 : (a, A) \cdot N_1) = \rho_{\text{FR}}(N_0, N_1)$ . It follows that the Fisher-Rao geodesics in  $\mathcal{N}$  are equivariant [31, 49]  $\gamma_{\text{FR}}^{\mathcal{N}}(B \cdot N_0, B \cdot N_1; t) = B \cdot \gamma_{\text{FR}}^{\mathcal{N}}(N_0, N_1; t)$  for any  $B \in \text{Aff}_+(d, \mathbb{R})$  and we can therefore consider without loss of generality that  $N_0$  is the standard normal distribution and  $N_1 \rightarrow N'_1 = N(\Sigma_0^{-\frac{1}{2}}(\mu_1, -\mu_0), \Sigma_0^{-\frac{1}{2}}\Sigma_1\Sigma_0^{-\frac{1}{2}})$ .

## 2.2 Fisher-Rao geodesics with boundary conditions

The Fisher-Rao geodesic Ordinary Differential Equation (ODE) for MVNs was first studied by Skovgaard [67]:

$$\begin{cases} \ddot{\mu} - \dot{\Sigma}\Sigma^{-1}\dot{\mu} & = 0, \\ \ddot{\Sigma} + \dot{\mu}\dot{\mu}^\top - \dot{\Sigma}\Sigma^{-1}\dot{\Sigma} & = 0. \end{cases} \quad (7)$$

Eriksen [31] first reported a solution of the geodesic equation with initial conditions: That is Fisher-Rao geodesics emanating from source  $N_0$  with initial prescribed tangent vector  $v_0 = \dot{\gamma}(0)$  in the tangent plane  $T_{N_0}$ . The initial tangent vector  $v_0 = (a_0, B_0) \in T_{N_0}$  consists of a vector part  $a_0$  and a symmetric matrix part  $B_0$ . Eriksen's solution required to compute a matrix exponential of a matrix of size  $(2d+1) \times (2d+1)$  and the inner use of square matrices of dimension  $2d+1$  was not fully geometrically elucidated [45]. See Appendix A.1 for details of Eriksen's method which gives a pregeodesic  $\underline{\gamma}_{\text{FR}}^{\mathcal{N}}(N_0, v_0; u)$  and not a geodesic  $\gamma_{\text{FR}}^{\mathcal{N}}(N_0, v_0; t)$  which is parameterized by arclength (constant speed). Geodesics can be obtained from pregeodesics by smooth reparameterization with an auxiliary function  $u(\cdot)$ :  $\gamma_{\text{FR}}^{\mathcal{N}}(N_0, v_0; t) = \underline{\gamma}_{\text{FR}}^{\mathcal{N}}(N_0, v_0; u(t))$ .

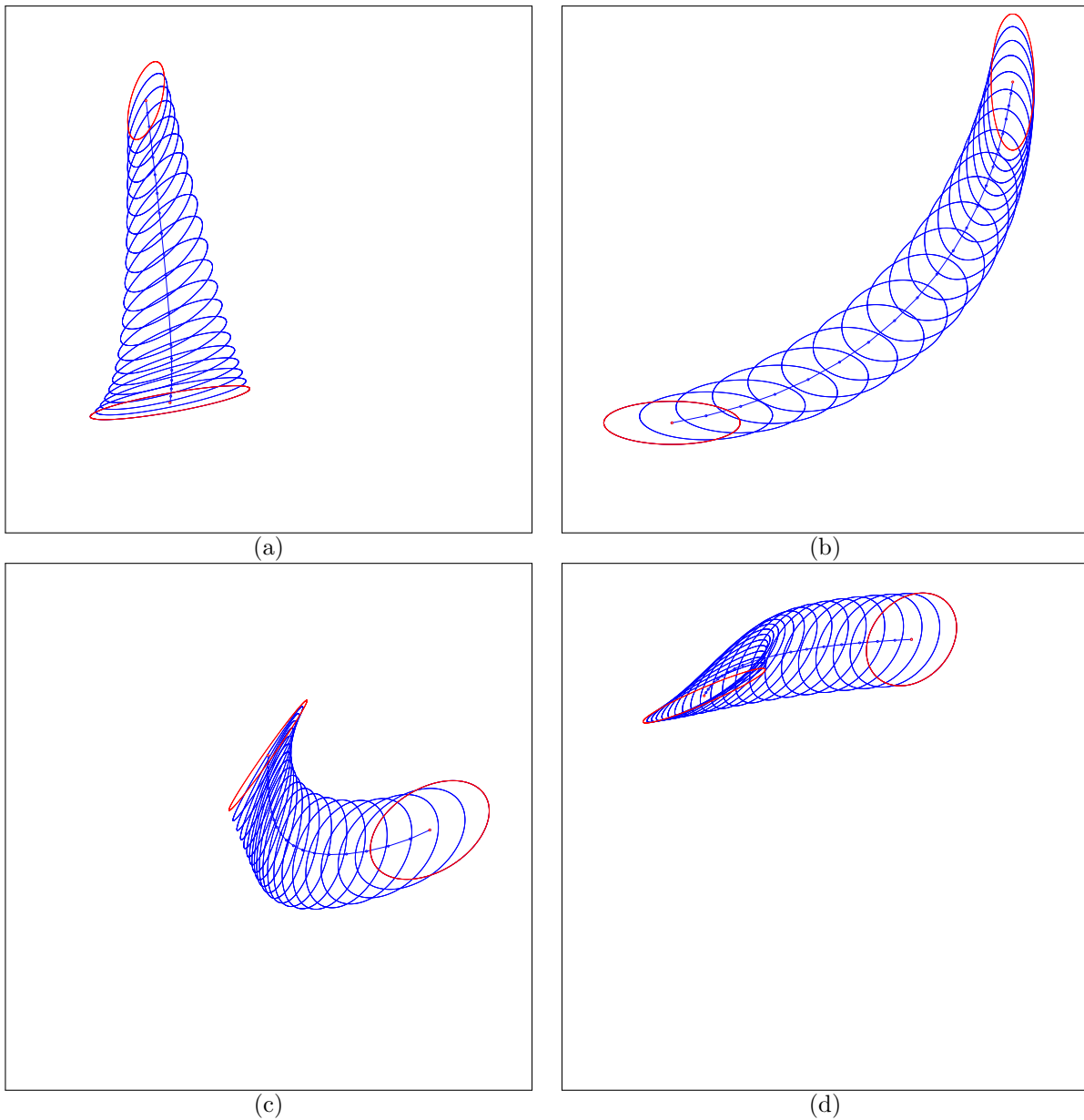


Figure 1: Some Fisher-Rao geodesics  $\gamma_{\text{FR}}^{\mathcal{N}}(N_0, N_1)$  with boundary conditions (bivariate normals  $N_0$  and  $N_1$  indicated by ellipsoids displayed in red) on the bivariate Gaussian manifold. The sample space  $\mathbb{R}^2$  is visualized for the range  $[-0.3, 1.2] \times [-0.3, 1.2]$ .

Calvo and Oller [21] later studied a more general differential equation system than in Eq. 7 and reported a closed-form solution without using extra dimensions (see Appendix A.2). For many years, the Fisher-Rao geodesics with boundary conditions  $N_0$  and  $N_1$  were not known in closed-form and had to be approximated using geodesic shooting methods [40, 61]: Those geodesic shooting methods were time consuming and numerically unstable, thus limiting their use in applications [40]. A recent breakthrough by Kobayashi [49] full explains and extends geometrically the rationale of Eriksen and obtains a method to compute in closed-form the Fisher-Rao geodesic with boundary conditions. Namely, Kobayashi [49] proved that the Fisher-Rao geodesics can be obtained by a Riemannian submersion of horizontal geodesics of the non-compact Riemannian symmetric space of dimension  $2d + 1$ . We report concisely below the recipe which we extracted from Kobayashi's principled geometric method to derive  $N_t = \gamma_{\text{FR}}^{\mathcal{N}}(N_0, N_1; t)$  as follows:

Algorithm 1. Fisher-Rao geodesic  $N_t = N(\mu(t), \Sigma(t)) = \gamma_{\text{FR}}^{\mathcal{N}}(N_0, N_1; t)$ :

- For  $i \in \{0, 1\}$ , let  $G_i = M_i D_i M_i^\top$ , where

$$D_i = \begin{bmatrix} \Sigma_i^{-1} & 0 & 0 \\ 0 & 1 & 0 \\ 0 & 0 & \Sigma_i \end{bmatrix}, \quad (8)$$

$$M_i = \begin{bmatrix} I_d & 0 & 0 \\ \mu_i^\top & 1 & 0 \\ 0 & -\mu_i & I_d \end{bmatrix}, \quad (9)$$

where  $I_d$  denotes the identity matrix of shape  $d \times d$ . That is, matrices  $G_0$  and  $G_1 \in \text{Sym}_+(2d + 1, \mathbb{R})$  can be expressed by *block Cholesky factorizations*.

- Consider the Riemannian geodesic in  $\text{Sym}_+(2d + 1, \mathbb{R})$  with respect to the trace metric:

$$G(t) = G_0^{\frac{1}{2}} \left( G_0^{-\frac{1}{2}} G_1 G_0^{-\frac{1}{2}} \right)^t G_0^{\frac{1}{2}}.$$

In order to compute the matrix power  $G^p$  for  $p \in \mathbb{R}$ , we first calculate the Singular Value Decomposition (SVD) of  $G$ :  $G = O L O^\top$  (where  $O$  is an orthogonal matrix and  $L = \text{diag}(\lambda_1, \dots, \lambda_{2d+1})$  a diagonal matrix) and then get the matrix power as  $G^p = O L^p O^\top$  with  $L^p = \text{diag}(\lambda_1^p, \dots, \lambda_{2d+1}^p)$ .

- Retrieve  $N(t) = \gamma_{\text{FR}}^{\mathcal{N}}(N_0, N_1; t) = N(\mu(t), \Sigma(t))$  from  $G(t)$ :

$$\Sigma(t) = [G(t)]_{1:d,1:d}^{-1}, \quad (10)$$

$$\mu(t) = \Sigma(t) [G(t)]_{1:d,d+1}, \quad (11)$$

where  $[G]_{1:d,1:d}$  denotes the block matrix with rows and columns ranging from 1 to  $d$  extracted from  $(2d + 1) \times (2d + 1)$  matrix  $G$ , and  $[G]_{1:d,d+1}$  is similarly the column vector of  $\mathbb{R}^d$  extracted from  $G$ .

Appendix E provides the Java™ source code.

Note that this technique also proves that the MVN geodesics are unique although  $\mathcal{N}$  is not NPC. It is proven in [34] that the Gaussian manifold admits a solvable Lie group and hence is diffeomorphic to some Euclidean space. Figure 1 displays several bivariate normal Fisher-Rao geodesics with boundary conditions obtained by implementing this method [49]. We display  $N(\mu, \Sigma)$  by an ellipse  $\mathcal{E} = \{\mu + Lx : \|x\|_2 = 1\}$  where  $\Sigma = LL^\top$  (Cholesky decomposition).

## 2.3 Fisher-Rao distances

### 2.3.1 Approximating Fisher-Rao lengths of curves

The previous section reported the closed-form solutions for the Fisher-Rao geodesics  $\gamma_{\text{FR}}^{\mathcal{N}}(N_0, N_1; t)$ . We shall now explain a method to approximate their lengths and hence the Fisher-Rao distances:

$$\rho_{\text{FR}}(N_0, N_1) = \text{Len}(\gamma_{\text{FR}}^{\mathcal{N}}(N_0, N_1; t)).$$

Consider discretizing regularly  $t \in [0, 1]$  using  $T + 1$  steps:  $\frac{0}{T} = 0, \frac{1}{T}, \dots, \frac{T-1}{T}, \frac{T}{T} = 1$ . Since geodesics are totally 1D submanifolds, we have

$$\rho_{\text{FR}}(N_0, N_1) = \sum_{i=0}^{T-1} \rho_{\text{FR}}(\gamma_{\text{FR}}(N_{\frac{i}{T}}, N_{\frac{i+1}{T}})).$$

By choosing  $T$  large enough, we have  $N = N_{\frac{i}{T}}$  close to  $N' = N_{\frac{i+1}{T}}$ , and we can approximate the geodesic distance as follows:

$$\rho_{\text{FR}}(N, N') \approx \text{ds}_{\text{Fisher}}(N) \approx \sqrt{\frac{2}{f''(1)} I_f(N, N')},$$

where  $I_f(p, q)$  is *any*  $f$ -divergence [3, 27] between pdfs  $p(x)$  and  $q(x)$  induced by a strictly convex generator  $f(u)$  satisfying  $f(1) = 0$ :

$$I_f(p, q) = \int p(x) f\left(\frac{q(x)}{p(x)}\right) dx.$$

Indeed, we have for two close distributions  $p_\theta$  and  $p_{\theta+d\theta}$  [5]:  $I_f(p_\theta, p_{\theta+d\theta}) \approx \frac{f''(1)}{2} \text{ds}_{\text{Fisher}}^2$ .

We choose the Jeffreys  $f$ -divergence which is the arithmetic symmetrization of the Kullback-Leibler divergence obtained for the generator  $f_J(u) = (u - 1) \log u$  with  $f_J''(1) = 2$ . It follows that  $D_J(N_1, N_2) = I_{f_J}(N_1, N_2) = \text{tr}\left(\frac{\Sigma_2^{-1}\Sigma_1 + \Sigma_1^{-1}\Sigma_2}{2} - I\right) + (\mu_2 - \mu_1)^\top \frac{\Sigma_1^{-1} + \Sigma_2^{-1}}{2} (\mu_2 - \mu_1)$ .

Thus we get the following overall approximation of the Fisher-Rao distance:

$$\tilde{\rho}_T(N_0, N_1) = \sum_{i=0}^{T-1} \sqrt{D_J\left(N_{\frac{i}{T}}, N_{\frac{i+1}{T}}\right)} \approx \rho_{\text{FR}}(N_0, N_1). \quad (12)$$

In [35], the authors choose  $\text{ds}_{\text{Fisher}}(p) = \sqrt{2D_{\text{KL}}(p_\theta, p_{\theta+d\theta})}$  where  $D_{\text{KL}} = I_{f_{\text{KL}}}$  is the Kullback-Leibler divergence, a  $f$ -divergence obtained for  $f_{\text{KL}}(u) = -\log u$ .

*Property 1* (Fisher-Rao upper bound). The Fisher-Rao distance between normal distributions is upper bounded by the square root of the Jeffreys divergence:  $\rho_{\text{FR}}(N_0, N_1) \leq \sqrt{D_J(N_0, N_1)}$ .

The proof can be found in many places, e.g. [39, 5, 65]. Yet we report another proof in Appendix B.

Notice that we have  $\rho_{\text{FR}}(N_0, N_1) \leq \tilde{\rho}_T(N_0, N_1)$  for all  $T > 1$ . Define the energy of a curve  $c(t)$  with  $t \in [a, b]$  by  $E(c) = \int_a^b \text{ds}_{\text{Fisher}}^2(t) dt$ . We have

$$E(\gamma_e^{\mathcal{N}}(N_0, N_1; t)) = E(\gamma_m^{\mathcal{N}}(N_0, N_1; t)) = D_J(N_0, N_1),$$

where  $\gamma_e^{\mathcal{N}}(N_0, N_1; t) = N(\mu_t^e, \Sigma_t^e)$  and  $\gamma_m^{\mathcal{N}}(N_0, N_1; t) = N(\mu_t^m, \Sigma_t^m)$  are the exponential and mixture geodesics in information geometry [77] given by  $\mu_t^m = \bar{\mu}_t$  and  $\Sigma_t^m = \bar{\Sigma}_t + t\mu_1\mu_1^\top + (1-t)\mu_2\mu_2^\top - \bar{\mu}_t\bar{\mu}_t^\top$  where  $\bar{\mu}_t = t\mu_1 + (1-t)\mu_2$  and  $\bar{\Sigma}_t = t\Sigma_1 + (1-t)\Sigma_2$ , and  $\mu_t^e = \bar{\Sigma}_t^H(t\Sigma_1^{-1}\mu_1 + (1-t)\Sigma_2^{-1}\mu_2)$  and  $\Sigma_t^e = \bar{\Sigma}_t^H$  where  $\bar{\Sigma}_t^H = (t\Sigma_1^{-1} + (1-t)\Sigma_2^{-1})^{-1}$  is the matrix harmonic mean. See Figure 3. The mixture, Fisher-Rao, and exponential geodesics are  $\alpha$ -connection geodesics [34] for  $\alpha = -1$ ,  $\alpha = 0$  and  $\alpha = 1$ , respectively. Notice that these e/m geodesics are computationally less intensive to evaluate than the Fisher-Rao geodesics. Figure 2 displays an example of the Fisher-Rao geodesics and the dual e/m geodesics between univariate normal distributions.

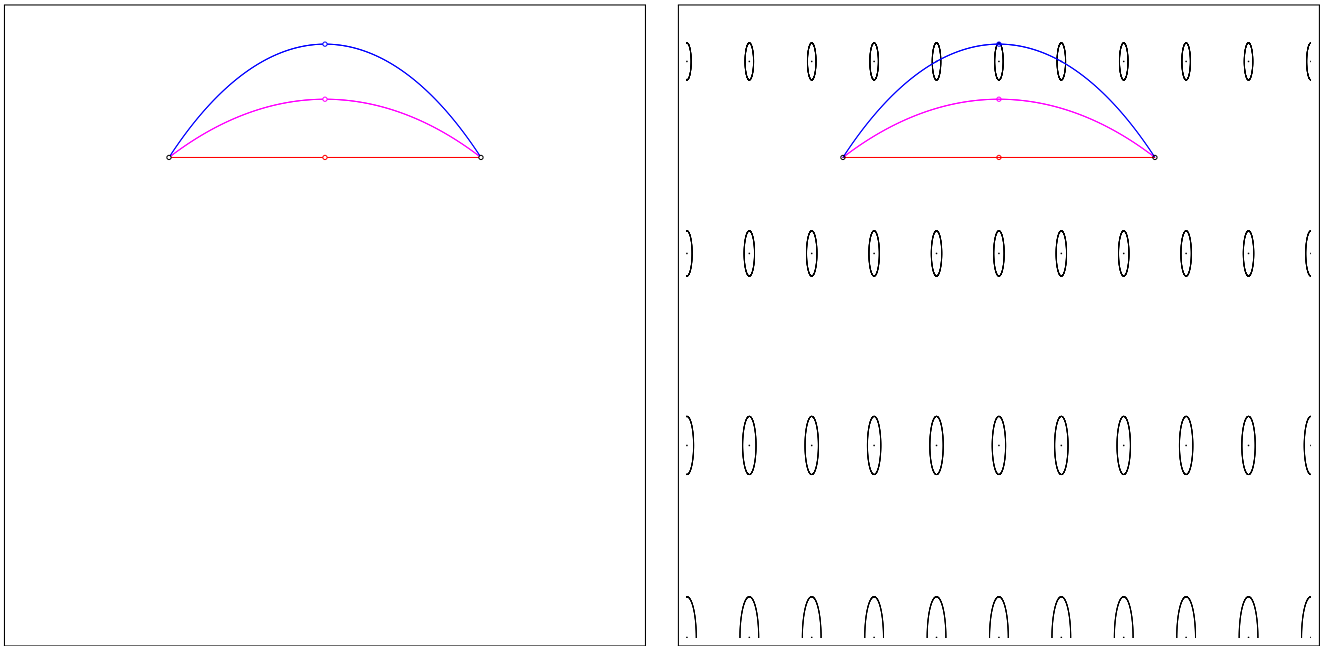


Figure 2: Visualizing on the upper plane  $(\mu, \sigma)$  the Fisher-Rao geodesic (purple), and dual exponential geodesic (red) and mixture geodesic (blue) between univariate normal distributions  $N_0 = N(0, 1)$  and  $N_1 = N(1, 1)$ . Left: geodesics with their corresponding midpoints. Right: same as Left with Tissot indicatrices shown

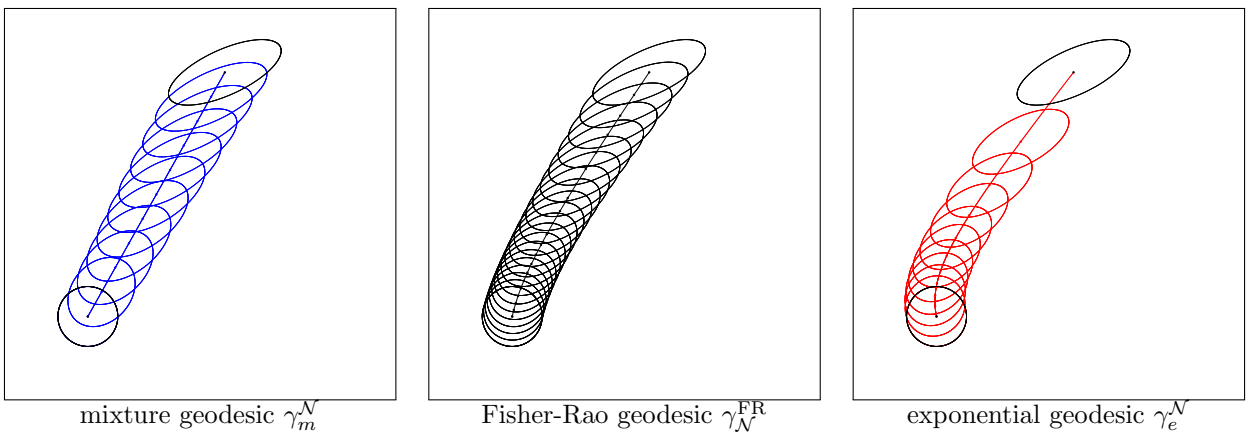


Figure 3: Visualizing geodesics with respect to the mixture, Levi-Civita (Fisher-Rao), and exponential connections.



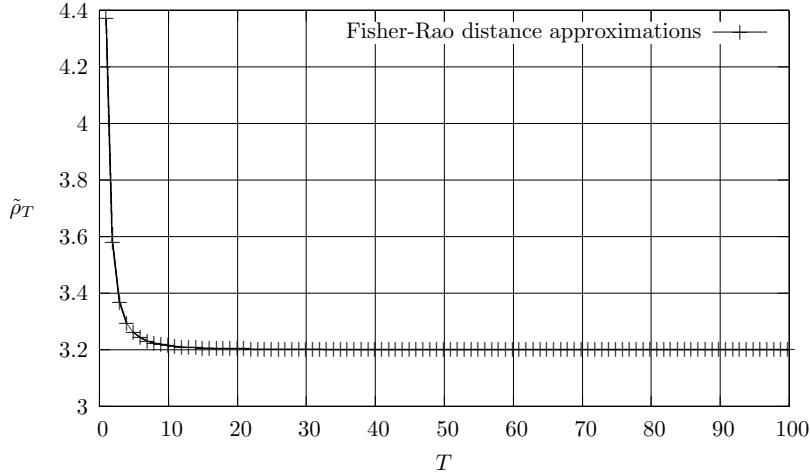


Figure 4: Convergence of  $\tilde{\rho}_T(N_0, N_1)$  to  $\rho_{\text{FR}}(N_0, N_1)$ .

Since the upper bound of Property 1 is tight infinitesimally, we get in the limit convergence to the Fisher-Rao distance:

$$\lim_{T \rightarrow \infty} \tilde{\rho}_T(N_0, N_1) = \rho_{\text{FR}}(N_0, N_1).$$

*Example 1.* Let us consider the example of Han and Park [40] (displayed in Figure 1(b)):

$N_0 = N\left(\begin{bmatrix} 0 \\ 0 \end{bmatrix}, \begin{bmatrix} 1 & 0 \\ 0 & 0.1 \end{bmatrix}\right)$  and  $N_1 = N\left(\begin{bmatrix} 1 \\ 1 \end{bmatrix}, \begin{bmatrix} 0.1 & 0 \\ 0 & 1 \end{bmatrix}\right)$ . The time consuming geodesic shooting algorithm of [40] evaluates the Fisher-Rao distance to  $\rho_{\mathcal{N}}(N_0, N_1) \approx 3.1329$ . We get the following approximations:  $\tilde{\rho}_T(N_0, N_1) = 3.1996$  for  $T = 100$ . See Figure 4 for the convergence curve of  $\tilde{\rho}_T(N_0, N_1)$  as a function of  $T$ .

A lower bound for the Fisher-Rao MVN distance between MVNs was given in [20] by using a Fisher isometric embedding into the SPD cone of dimension  $d + 1$ . Calvo and Oller [20] showed that mapping  $N = N(\mu, \Sigma)$  by

$$\bar{N} = f(N) := \begin{bmatrix} \Sigma + \mu\mu^\top & \mu \\ \mu^\top & 1 \end{bmatrix} \in \mathcal{P}(d+1), \quad (13)$$

embeds the Gaussian manifold into a submanifold  $\bar{\mathcal{N}}$  in the SPD cone  $\mathcal{P}(d+1)$  of codimension 1. Moreover, when  $\mathcal{P}(d+1)$  is equipped with half the trace metric  $\frac{1}{2}g_{\text{trace}}$ , the embedded MVN submanifold is Fisher isometric. However, the submanifold  $\bar{\mathcal{N}}$  is not totally geodesic. Thus by taking the Riemannian SPD distance in  $\mathcal{P}(d+1)$  induced by  $\frac{1}{2}g_{\text{trace}}$ , we get a lower bound on the Fisher-Rao distance:

$$\rho_{\text{CO}}(N_0, N_1) = \frac{1}{\sqrt{2}} \sum_{i=1}^{d+1} \log^2 \lambda_i(\bar{\mathcal{N}}_0^{-\frac{1}{2}} \bar{\mathcal{N}}_1 \bar{\mathcal{N}}_0^{-\frac{1}{2}}).$$

**Proposition 2.1.** *A lower bound on the Fisher-Rao distance between  $N_0 = N(\mu_0, \Sigma_0)$  and  $N_1 = N(\mu_1, \Sigma_1)$  is*

$$\rho_{\text{CO}}(N_0, N_1) = \frac{1}{\sqrt{2}} \sum_{i=1}^{d+1} \log^2 \lambda_i(\bar{\mathcal{N}}_0^{-\frac{1}{2}} \bar{\mathcal{N}}_1 \bar{\mathcal{N}}_0^{-\frac{1}{2}}),$$

where  $\bar{N}_i = \begin{bmatrix} \Sigma_i + \mu_i\mu_i^\top & \mu_i \\ \mu_i^\top & 1 \end{bmatrix}$  for  $i \in \{0, 1\}$ , and the  $\lambda_i(M)$ 's denote the eigenvalues of matrix  $M$ .

Notice that by Nash embedding theorems, any Riemannian manifold  $(M, g)$  can be embedded as a submanifold of the Euclidean manifold of higher dimension.

### 2.3.2 A guaranteed $(1 + \epsilon)$ -approximation of the Fisher-Rao MVN distance

Using the lower and upper bounds on the Fisher-Rao distance and the closed-form solution for the Fisher-Rao geodesics with boundary value conditions, we can design a guaranteed  $(1 + \epsilon)$ -approximation recursive algorithm for the Fisher-Rao MVN distance as follows:

Algorithm 2.  $\tilde{\rho}_{\text{FR}}(N_0, N_1) = \text{ApproximateRaoMVN}(N_0, N_1, \epsilon)$ :

- $l = \rho_{\text{CO}}(N_0, N_1)$ ; /\* Calvo & Oller lower bound (Proposition 2.1) \*/
- $u = \sqrt{D_J(N_0, N_1)}$ ; /\* Jeffreys divergence  $D_J$  (Proposition 1) \*/
- if  $(\frac{u}{l} > 1 + \epsilon)$ 
  - $N = \text{GeodesicMidpoint}(N_0, N_1)$ ; /\* see Algorithm 1 for  $t = \frac{1}{2}$ . \*/
  - return  $\text{ApproximateRaoMVN}(N_0, N, \epsilon) + \text{ApproximateRaoMVN}(N, N_1, \epsilon)$ ;
- else return  $u$ ;

**Theorem 2.2.** *We can compute a  $(1 + \epsilon)$ -approximation of the Fisher-Rao distance between two multivariate normal distributions for any  $\epsilon > 0$ .*

*Proof.* The proof follows from the fact that when  $\frac{u}{l} \leq 1 + \epsilon$  then we have

$$\sqrt{D_J(N_0, N_1)} \leq (1 + \epsilon)\rho_{\text{CO}}(N_0, N_1) \leq (1 + \epsilon)\rho_{\text{FR}}(N_0, N_1).$$

Since we cut recursively along the geodesics  $\gamma_{\text{FR}}(N_0, N_1)$  into overall  $T + 1$  pieces  $N_{\frac{i}{T}}$ , we have

$$\tilde{\rho}_{\text{FR}}(N_0, N_1) = \sum_{i=0}^{T-1} \tilde{\rho}(N_{\frac{i}{T}}, N_{\frac{i+1}{T}}) \leq \sum_{i=0}^{T-1} (1 + \epsilon)\rho_{\text{FR}}((N_{\frac{i}{T}}, N_{\frac{i+1}{T}})).$$

But  $\gamma_{\text{FR}}(N_0, N_1)$  is totally geodesic so that  $\sum_{i=0}^{T-1} \rho_{\text{FR}}((N_{\frac{i}{T}}, N_{\frac{i+1}{T}})) = \rho_{\text{FR}}(N_0, N_1)$ . It follows that

$$\tilde{\rho}_{\text{FR}}(N_0, N_1) \leq (1 + \epsilon)\rho_{\text{FR}}(N_0, N_1).$$

□

Instead of computing exactly the geodesic midpoint  $\gamma_{\text{FR}}(N_0, N_1; \frac{1}{2})$ , we may use the matrix arithmetic-harmonic mean algorithm of [55] which convergence quadratically to the geometric matrix mean of  $\bar{N}_0$  and  $\bar{N}_1$  (i.e., the geodesic midpoint). The matrix AHM only requires to compute matrix inverses for calculating the matrix harmonic means (see Appendix C).

Figure 5 shows the discretization steps of the Fisher-Rao geodesic between two bivariate normal distributions for  $\epsilon \in \{0.1, 0.01, 0.001, 0.0001\}$  with the number of control points on the geodesics and the guaranteed  $(1 + \epsilon)$ -approximation of the Fisher-Rao distance. Figure 6 illustrates several examples of discretized Fisher-Rao geodesics between bivariate normal distributions obtained for  $\epsilon = 0.01$ .

## 3 Fisher-Rao clustering

We shall consider two applications of the Fisher-Rao distance between MVNs using clustering:

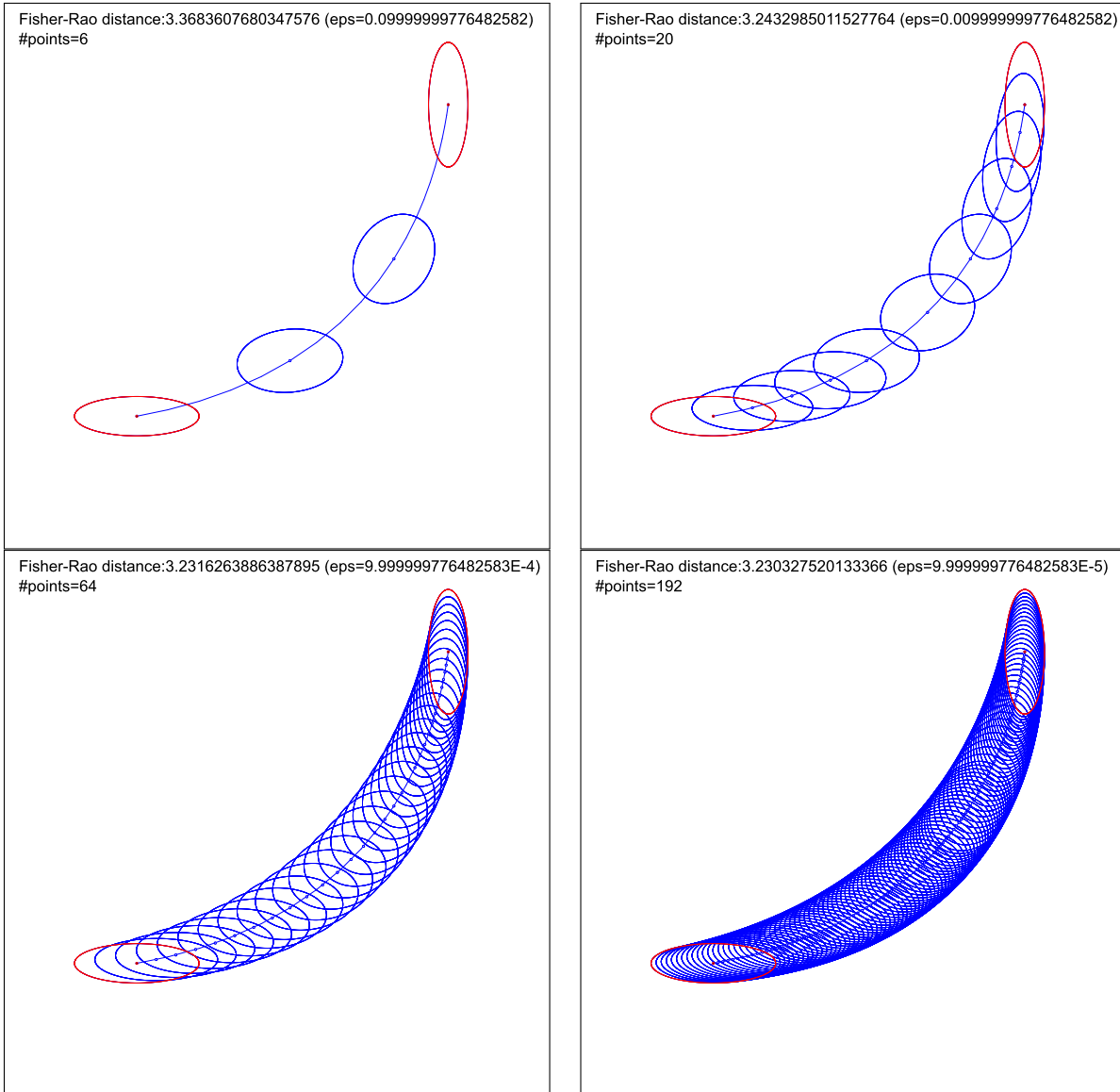


Figure 5: Some discretizations of the Fisher-Rao geodesics between two bivariate normals guaranteeing a  $(1 + \epsilon)$ -approximation of the Fisher-Rao distance for  $\epsilon \in \{0.1, 0.01, 0.001, 0.0001\}$ .

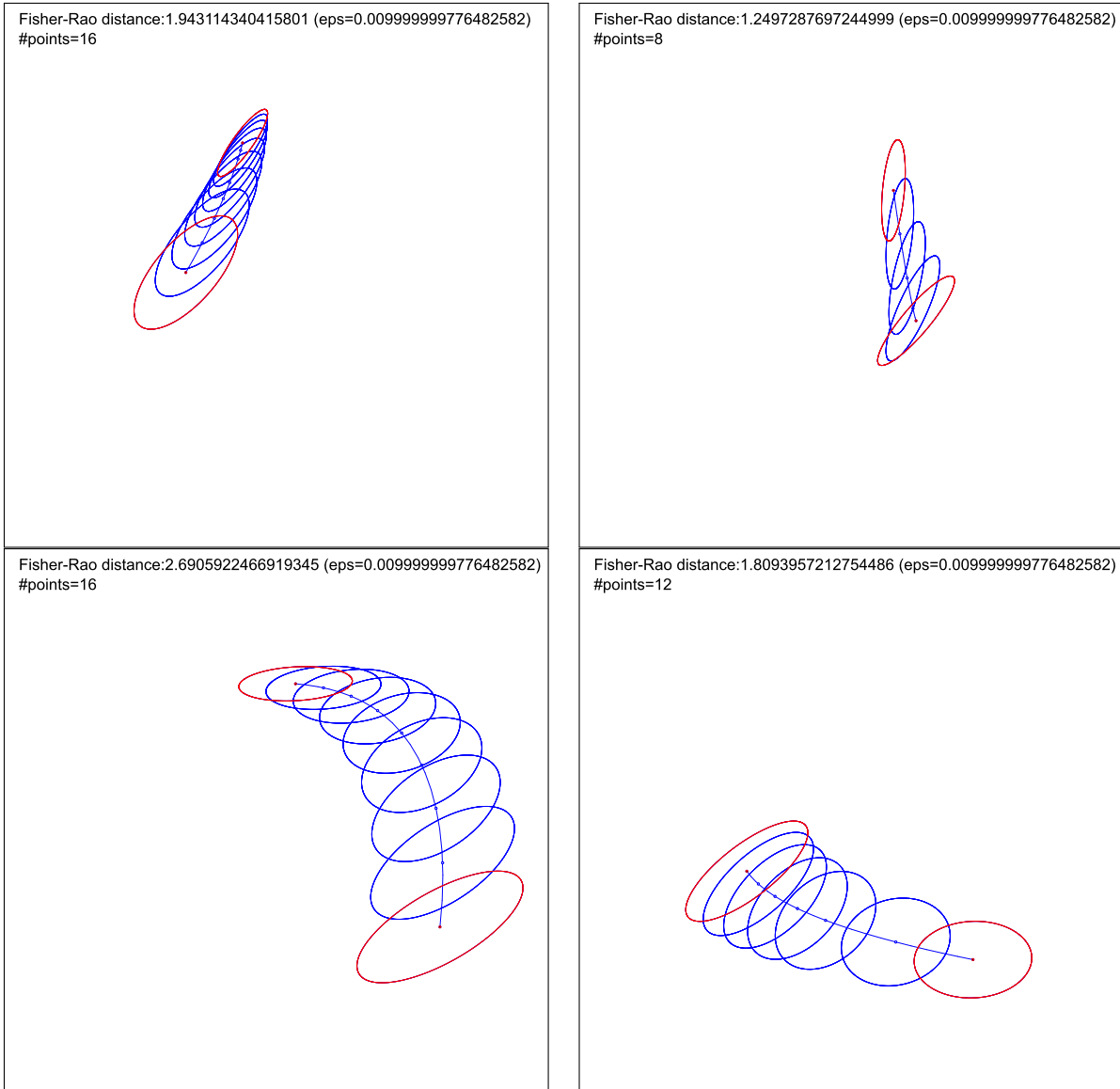


Figure 6: Some discretizations of the Fisher-Rao geodesics between two random bivariate normals guaranteeing a  $(1 + \epsilon)$ -approximation of the Fisher-Rao distance for  $\epsilon = 0.01$ .

The first application considers clustering weighted MVNs which is useful to simplify Gaussian Mixture Models [28, 69] (GMMs): A GMM  $m(x) = \sum_{i=1}^n w_i p_{\mu_i, \Sigma_i}(x)$  with  $n$  components is a weighted set of  $n$  MVNs  $N(\mu_i, \Sigma_i)$  and clustering this set into  $k$ -clusters allows one to simplify the GMM  $m(x)$ . For this task, we may use the  $k$ -means clustering [53] when centroids are available in closed-form [28] (using the Kullback-Leibler divergence) or the  $k$ -mediod clustering [48] when we choose the representative of clusters from the input otherwise (using the Fisher-Rao distance).

The second application considers the quantization of sets of MVNs which is useful to further compress a set  $\{m_1, \dots, m_n\}$  of  $n$  GMMs  $m_i(x) = \sum_{j=1}^{n_i} w_{i,j} p_{\mu_{i,j}, \Sigma_{i,j}}(x)$  with overall  $N = \sum_{i=1}^n n_i$  MVNs  $N(\mu_{i,j}, \Sigma_{i,j})$ . We build a codebook of  $k$  MVNs  $N(m_i, S_i)$  by quantizing the  $N$  non-weighted MVNs using the guaranteed  $k$ -center clustering of [38] (also called  $k$ -centers clustering [30]). Then each mixture  $m_i(x)$  is quantized into a mixture  $\tilde{m}_{w_i}(x) = \sum_{i=1}^k w_{i,j} p_{m_i, S_i}(x)$ . The advantage of quantization is that the original set  $\{m_1, \dots, m_n\}$  of GMMs is compactly represented by  $n$  points in the  $(k-1)$ -dimensional standard simplex  $\Delta_{k-1}$  encoding  $\{\tilde{m}_1, \dots, \tilde{m}_n\}$  since they share the same components. The set  $\{\tilde{m}_w : w \in \Delta_{k-1}\}$  form a mixture family in information geometry [5, 57] with a dually flat space which can be exploited algorithmically.

Notice that minimizing the objective functions of these  $k$ -means,  $k$ -mediod and  $k$ -center clustering objective are NP-hard when dealing with MVNs.

### 3.1 Nearest neighbor queries

In order to speed up these center-based clustering, we shall find for a given MVN  $N(\mu, \Sigma)$  (a query) its closest cluster center among  $k$  MVNs  $\{N(m_i, S_i)\}$  using Nearest Neighbor (NN) query search [6, 12]. There exist many data-structures for exact and approximate NN queries. For example, the vantage point (VP) tree structure is well-suited in metric spaces [76] and has also been considered for NN queries with respect to the Kullback-Leibler divergence between MVNs [58]. Although NN queries based on VP-trees still require linear time in the worst-case, they can also achieve logarithmic time in best cases. At the heart of NN search using VP-trees, we are given a query ball  $\text{Ball}(p, r)$  with center  $p$  and radius  $r$ , and we need to find potential intersections with balls  $\text{Ball}(v, r_v)$  stored at nodes  $v$  of the VP tree. Thus when using the (fine approximation  $\tilde{\rho}_T$ ) Fisher-Rao metric distance, we need to answer predicates of whether two Fisher-Rao balls  $\text{Ball}_{\text{FR}}(N, r)$  and  $\text{Ball}_{\text{FR}}(N', r')$  intersect or not: This can be done by determining the sign of  $\rho_{\text{FR}}(N, N') - (r + r')$ . When positive the balls do not intersect and when negative the balls intersect. Since we handle some approximation errors by using  $\tilde{\rho}_T$  instead of  $\rho_{\text{FR}}$ , but since  $\tilde{\rho}_T \geq \rho_{\text{FR}}$  we need to explore both branches of a VP-tree if the balls  $\text{Ball}_{\text{FR}}(N, r)$  and  $\text{Ball}_{\text{FR}}(N', r')$  stored at the two siblings of a node  $v$  are such that  $\tilde{\rho}_T(N, N') \leq r + r'$ .

### 3.2 $k$ -centers clustering and miniball

For the quantization tasks, the  $k$ -center clustering heuristic of Gonzalez [38] guarantees to find a good  $k$ -center clustering in metric spaces with an approximation factor upper bounded by 2. We can further refine the cluster representative of each cluster by computing approximations of the *smallest enclosing Fisher-Rao balls* (miniballs) of clusters.

A simple Riemannian approximation technique has been reported for approximating the smallest enclosing ball of  $n$  points  $\{p_1, \dots, p_n\}$  on a Riemannian manifold  $(M, g)$  with geodesic distance  $\rho_g(p, p')$  and geodesics  $\gamma_g(p, p'; t)$  in [7]:

Miniball $(\{p_1, \dots, p_n\}, \rho_g, T)$ :

- Let  $c_1 \leftarrow p_1$
- For  $t = 1$  to  $T$ 
  - Compute the index of the point which is farthest to current circumcenter  $c_t$ :

$$f_t = \arg \max_{i \in \{1, \dots, n\}} \rho_g(c_t, p_i)$$

- Update the circumcenter by walking along the geodesic linking  $c_t$  to  $p_{f_t}$ :

$$c_{t+1} = \gamma_g \left( c_t, p_{f_t}; \frac{1}{t+1} \right)$$

Recall that geodesics are parameterized by normalized arc length so that  $\rho_g(c_t, c_{t+1}) = \frac{1}{t+1} \rho_g(c_t, p_{f_t})$ .

- Return  $c_T$

Conditions of convergence are analyzed in [7]: For example, it always converge for Cartan-Hadamard manifolds (complete simply connected NPC manifolds like the SPD cone).

The Fisher-Rao distance  $\rho_{\text{FR}}(N_{\Sigma}(\mu_0), N_{\Sigma}(\mu_1))$  between two MVNs with same covariance matrix  $\Sigma$  is

$$\rho_{\text{FR}}(N_{\Sigma}(\mu_0), N_{\Sigma}(\mu_1)) = \sqrt{2} \operatorname{arccosh} \left( 1 + \frac{1}{4} \Delta_{\Sigma}^2(\mu_0, \mu_1) \right),$$

where  $\Delta_{\Sigma}(\mu_0, \mu_1) = \sqrt{(\mu_0 - \mu_1)^{\top} \Sigma^{-1} (\mu_0 - \mu_1)}$  is the Mahalanobis distance. Therefore when all MVNs belong to the non-totally flat submanifold  $\mathcal{N}_{\Sigma} = \{N(\mu, \Sigma) : \mu \in \mathbb{R}^d\}$ , the smallest enclosing ball amounts to an Euclidean smallest enclosing ball [75] since in that case  $\rho_{\text{FR}}$  is an increasing function of the Mahalanobis distance.

Since the computations of  $\tilde{\rho}_T$  approximating  $\rho_{\text{FR}}$  is costly, the following section shall consider a new fast metric distance on  $\mathcal{N}$  which further relates to the Fisher-Rao distance.

## 4 Pullback Hilbert cone distance

Let us define dissimilarities and paths on  $\mathcal{N}(d)$  from dissimilarities and geodesics on  $\mathcal{P}(d+1) = \mathcal{N}_0(d)$  by considering the following family of *diffeomorphic embeddings*  $f_a : \mathcal{N}(d) \rightarrow \mathcal{P}(d+1)$  for  $a \in \mathbb{R}_{>0}$  proposed in [20]:

$$f_a(N(\mu, \Sigma)) := \begin{bmatrix} \Sigma + a\mu\mu^{\top} & a\mu \\ a\mu^{\top} & a \end{bmatrix} \in \mathcal{P}(d+1). \quad (14)$$

Let  $\overline{\mathcal{N}}_a(d) = \{f_a(N) : N \in \mathcal{N}(d)\} \subset \mathcal{P}(d+1)$  denote the embedded Gaussian submanifold in  $\mathcal{P}(d+1)$  of codimension 1 that is obtained by pushing the normals to SPD matrices (Figure 7). We let  $f_a^{\text{inv}} : \overline{\mathcal{N}}_a(d) \rightarrow \mathcal{N}(d)$  denote the functional inverse so that  $f_a \circ f_a^{\text{inv}} = \text{id}_{\mathcal{N}}$  is the identity function  $\text{id}_{\mathcal{N}} : \mathcal{N} \rightarrow \mathcal{N}$ . Function  $f_a^{\text{inv}}$  pulls back the SPD matrices to the normal distributions (Figure 7). The notation *inv* in  $f_a^{\text{inv}}$  is chosen to avoid confusion with the matrix inverse  $f_a(N(\mu, \Sigma))^{-1}$ :

$$f_a(N(\mu, \Sigma))^{-1} = \begin{bmatrix} \Sigma^{-1} & -\Sigma^{-1}\mu \\ -\mu^{\top}\Sigma^{-1} & \mu^{\top}\Sigma^{-1}\mu + \frac{1}{a} \end{bmatrix}.$$

The open SPD cone  $\mathcal{P}(d+1)$  can thus be foliated by the family of submanifolds  $\overline{\mathcal{N}}_a$  [20]:  $\mathcal{P}(d+1) = \{a \times \overline{\mathcal{N}}_a : a \in \mathbb{R}_{>0}\}$ . We let  $f = f_1$  and  $f^{\text{inv}} = f_1^{\text{inv}}$ , and  $\overline{\mathcal{N}} = \overline{\mathcal{N}}_1$ .

Calvo and Oller [20] proved that  $(\mathcal{N}(d), g_{\text{Fisher}})$  is isometrically embedded into  $(\mathcal{P}(d+1), \frac{1}{2}g_{\text{trace}})$  but that  $\overline{\mathcal{N}}$  is not totally geodesic. Thus we have

$$\begin{aligned} \rho_{\text{CO}}(N_0, N_1) &= \rho_{\text{FR}}(N(0, f(N_0)), N(0, f(N_1))), \\ &= \rho_{\mathcal{P}}(\overline{\mathcal{N}}_0, \overline{\mathcal{N}}_1) \geq \rho_{\text{FR}}(N_0, N_1), \end{aligned}$$

where  $\overline{\mathcal{N}}_i = f(N_i)$ . See Eq. 5. It follows that we get a series of lower bound for  $\rho_{\text{FR}}(N_0, N_1)$ :

$$\rho_{\text{CO}, T}(N_0, N_1) = \sum_{i=0}^{T-1} \rho_{\mathcal{P}} \left( N_{\frac{i}{T}}, N_{\frac{i+1}{T}} \right),$$

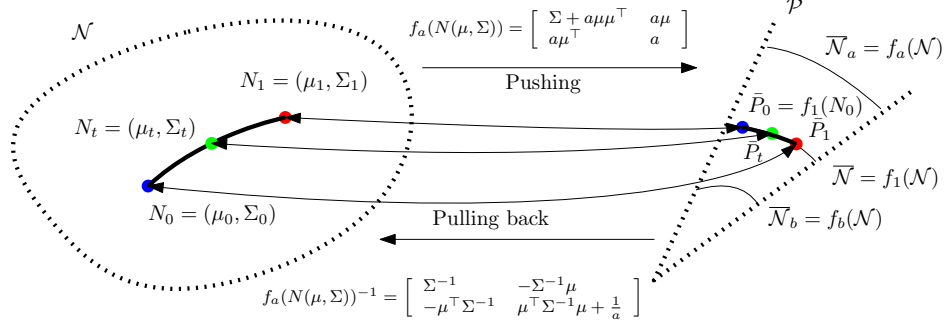


Figure 7: Pushing the  $d$ -dimensional normals  $\mathcal{N}$  to a submanifold  $\bar{\mathcal{N}}$  of the  $(d+1) \times (d+1)$ -dimensional SPD cone via a diffeomorphic embedding  $f$ , and pulling back a geodesic/curve on the SPD cone to the normal manifold with  $f^{-1}$ .

such that for all  $T$ ,  $\tilde{\rho}_T \geq \rho_{\text{FR}} \geq \rho_{\text{CO}, T}$ .

We can also approximate the smallest enclosing Fisher-Rao ball of  $\{N(\mu_i, \Sigma_i)\}$  on  $\mathcal{N}(d)$  by embedding the normals into  $\bar{\mathcal{N}}$  as  $\{\bar{P}_i = f(N(\mu_i, \Sigma_i))\}$ . We then apply the above iterative smallest enclosing ball approximation Miniball [7] to get  $\tilde{C}_T \in \mathcal{P}(d+1)$  after  $T$  iterations. Then we project orthogonally with respect to the trace metric  $\tilde{C}_T$  onto  $\bar{\mathcal{N}}$  as  $\bar{C}_T = \text{proj}_{\bar{\mathcal{N}}}(\tilde{C}_T)$  and maps back to the Gaussian manifold using  $f^{\text{inv}}$  to get the approximate normal circumcenter.

The following proposition describes the orthogonal projection operation  $\bar{P}_\perp = \text{proj}_{\bar{\mathcal{N}}}(P)$  of  $P = [P_{i,j}] \in \mathcal{P}(d+1)$  onto  $\bar{\mathcal{N}}$  based on the analysis reported in the Appendix of [20] (page 239):

**Proposition 4.1.** *Let  $\beta = P_{d+1, d+1}$  and write  $P = \begin{bmatrix} \Sigma + \beta\mu\mu^\top & \beta\mu \\ \beta\mu^\top & \beta \end{bmatrix}$ . Then the orthogonal projection at  $P \in \mathcal{P}$  onto  $\bar{\mathcal{N}}$  is:*

$$\bar{P}_\perp := \text{proj}_{\bar{\mathcal{N}}}(P) = \begin{bmatrix} \Sigma + \mu\mu^\top & \mu^\top \\ \mu & 1 \end{bmatrix}, \quad (15)$$

and the SPD trace distance between  $P$  and  $\bar{P}_\perp$  is

$$\rho_{\mathcal{P}}(P, \bar{P}_\perp) = |\log \beta|. \quad (16)$$

Consider pulling back SPD cone dissimilarities and geodesics of  $\mathcal{P}(d+1)$  onto  $\mathcal{N}(d)$  as follows:

**Definition 4.2** (Pullback dissimilarities). A dissimilarity  $D(N_0, N_1)$  (not necessarily be a metric distance nor a smooth divergence) on  $\mathcal{N}(d)$  (with  $N_0 := N(\mu_0, \Sigma_0)$  and  $N_1 := N(\mu_1, \Sigma_1)$ ) can be obtained from any dissimilarity  $D_{\text{SPD}}(\cdot, \cdot)$  on the SPD cone by pulling back the SPD matrix cone dissimilarity using  $f$ :

$$D(N_0, N_1) := D_{\text{SPD}}(f(N_0), f(N_1)). \quad (17)$$

Similarly, we pullback cone geodesics onto  $\mathcal{N}$ :

**Definition 4.3** (Pullback curves). A path  $c_\gamma(N_0, N_1; t)$  joining  $N_0 = c_\gamma(N_0, N_1; 0)$  and  $N_1 = c_\gamma(N_0, N_1; 1)$  can be defined by the pullback of any geodesic  $\gamma(f(N_0), f(N_1); t)$  on the SPD cone:

$$c_\gamma(N_0, N_1; t) := f^{\text{inv}}(\gamma(f(N_0), f(N_1); t)). \quad (18)$$

Hence, we can leverage the rich literature on dissimilarities and geodesics on the SPD cone (e.g., [41, 23, 68, 8, 24]). Note that the Riemannian SPD trace metric geodesic is also the geodesic for Finslerian distances  $\rho_h(P_0, P_1) := \left\| \text{Log} \left( P_0^{-\frac{1}{2}} P_1 P_0^{-\frac{1}{2}} \right) \right\|_h$  where  $h$  is a totally symmetric gauge function (i.e.,  $h(x_1, \dots, x_n) =$

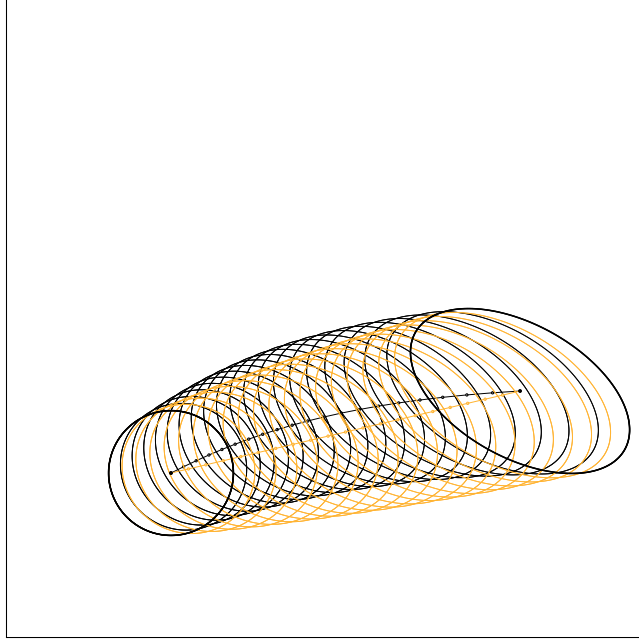


Figure 8: Comparing the pullback Hilbert geodesic (orange, coinciding with the mixture geodesic) with the exact Fisher-Rao geodesic displayed in black.

$h(\sigma(x_1, \dots, x_n))$  for any permutation  $\sigma$ ) and  $\|P\|_h := h(\lambda_1(P), \dots, \lambda_d(P))$ . When  $h(x) = h_p(x) = \|x\|_p = \left(\sum_{i=1}^d x_i^p\right)^{\frac{1}{p}}$  is the  $p$ -norm for  $1 \leq p < \infty$ , we get the Schatten matrix  $p$ -norms [13].

The *Hilbert projective distance* also called *Birkhoff projective distance* [42, 15, 24] on the SPD cone  $\text{Sym}_+(d, \mathbb{R})$  is defined by

$$\begin{aligned} \rho_{\text{Hilbert}}(P_0, P_1) &= \log \left( \frac{\lambda_{\max}(P_0^{-\frac{1}{2}} P_1 P_0^{-\frac{1}{2}})}{\lambda_{\min}(P_0^{-\frac{1}{2}} P_1 P_0^{-\frac{1}{2}})} \right), \\ &= \log \left( \frac{\lambda_{\max}(P_0^{-1} P_1)}{\lambda_{\min}(P_0^{-1} P_1)} \right). \end{aligned}$$

It is a *projective distance* (or quasi-metric distance) because it is symmetric and satisfies the triangular inequality but we have  $\rho_{\text{Hilbert}}(P_0, P_1) = 0$  if and only if  $P_0 = \lambda P_1$  for some  $\lambda > 0$ . It was proven in [50] (Theorem 4.1) that any projective distance with strict contraction ratio under linear mapping is necessarily a scalar function of the Hilbert's projective metric, and that the Hilbert projective distance has the lowest possible contraction ratio.

However, the pullback Hilbert distance on  $\mathcal{N}$ ,  $\rho_{\text{Hilbert}}(N_0, N_1) := \rho_{\text{Hilbert}}(f(N_0), f(N_1))$ , is a proper metric distance on  $\overline{\mathcal{N}}$  since  $f(N_0) = f(N_1)$  if and only if  $\lambda = 1$  because the array element at last row and last column  $[f(N_0)]_{d+1, d+1} = [f(N_1)]_{d+1, d+1} = 1$  is identical. Thus  $f(N_0) = \lambda f(N_1)$  for  $\lambda = 1$ . The pullback Hilbert cone distance only requires to calculate the *extreme eigenvalues* of the matrix product  $f(N_0)^{-1} f(N_1)$ . Thus we can bypass a costly SVD and compute approximately these extreme eigenvalues using the power method [72] (Appendix D).

The geodesic in the Hilbert SPD cone are straight lines [59] parameterized as follows:

$$\gamma_{\text{Hilbert}}(P_0, P_1; t) := \left( \frac{\beta \alpha^t - \alpha \beta^t}{\beta - \alpha} \right) P_0 + \left( \frac{\beta^t - \alpha^t}{\beta - \alpha} \right) P_1,$$



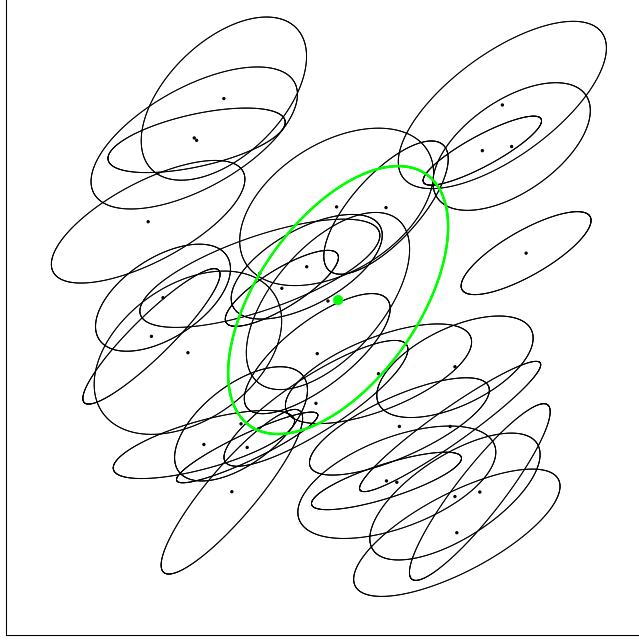


Figure 9: Approximating the Hilbert smallest enclosing ball of a set of bivariate normal distributions. The approximated minimax center is shown in green.

where  $\alpha = \lambda_{\min}(P_1^{-1}P_0)$  and  $\beta = \lambda_{\max}(P_1^{-1}P_0)$ . Figure 8 compares the pullback Hilbert geodesic curve with the Fisher-Rao geodesic.

A pregeodesic is a geodesic which may be arbitrarily reparameterized by another parameter  $u = r(t)$  for some smooth function  $r$ . That is, a pregeodesic is not necessarily parameterized by arc length. Let us notice that the weighted arithmetic mean  $\text{LERP}(P_0, P_1; u) = (1 - u)P_0 + uP_1$  is a pregeodesic of  $\gamma_{\text{Hilbert}}(P_0, P_1; t)$ . Although Hilbert SPD space is not a Riemannian space, it enjoys non-positive curvature properties according to various definitions of curvatures [2, 47].

We can adapt the approximation of the minimum enclosing Hilbert ball by replacing  $\rho_{\text{FR}}$  by  $\rho_{\text{Hilbert}}$  and cutting metric geodesic  $\gamma_{\text{Hilbert}}$  instead of geodesics  $\gamma_{\text{FR}}^{\mathcal{N}}$  (see Figure 9).

First, the diffeomorphic embedding  $f$  exhibits several interesting features:

**Proposition 4.4.** *The Jeffreys divergence between  $p_{\mu_1, \Sigma_1}$  and  $p_{\mu_2, \Sigma_2}$  amounts to the Jeffreys divergence between  $q_{\bar{P}_1} = p_{0, f(\mu_1, \Sigma_1)}$  and  $q_{\bar{P}_2} = p_{0, f(\mu_2, \Sigma_2)}$  where  $\bar{P}_i = f(\mu_i, \Sigma_i)$ :  $D_J(p_{\mu_1, \Sigma_1}, p_{\mu_2, \Sigma_2}) = D_J(q_{\bar{P}_1}, q_{\bar{P}_2})$ .*

*Proof.* Since  $D_J(p, q) = D_{\text{KL}}(p, q) + D_{\text{KL}}(q, p)$ , we shall prove that  $D_{\text{KL}}(p_{\mu_1, \Sigma_1}, p_{\mu_2, \Sigma_2}) = D_{\text{KL}}(q_{\bar{P}_1}, q_{\bar{P}_2})$ . The KLD between two centered  $(d + 1)$ -variate normals  $q_{P_1} = p_{0, P_1}$  and  $q_{P_2} = p_{0, P_2}$  is

$$D_{\text{KL}}(q_{P_1}, q_{P_2}) = \frac{1}{2} \left( \text{tr}(P_2^{-1}P_1) - d - 1 + \log \frac{|P_2|}{|P_1|} \right).$$

This divergence can be interpreted as the matrix version of the Itakura-Saito divergence [28]. It is a matrix spectral distance since we can write  $D_{\text{KL}}(q_{P_1}, q_{P_2}) = (h_{\text{KL}} \circ \lambda^{\text{SP}})(\Sigma_2^{-1}\Sigma_1)$ , where  $\lambda^{\text{SP}}(S) = (\lambda_1(S), \dots, \lambda_d(S))$  and  $h_{\text{KL}}(u_1, \dots, u_d) = \frac{1}{2} (u_i - 1 - \log u_i)$  (a gauge function). Similarly, the Jeffreys divergence between two centered MVNs is a matrix spectral distance with gauge function  $h_J(u) = \sum_{i=1}^d \left( \sqrt{u_i} - \frac{1}{\sqrt{u_i}} \right)^2$ .

The SPD cone equipped with  $\frac{1}{2}$  of the trace metric can be interpreted as Fisher-Rao centered normal manifolds (isometry):  $\forall \mu, (\mathcal{N}_\mu, g_{\mathcal{N}_\mu}^{\text{Fisher}}) \cong (\mathcal{P}, \frac{1}{2}g^{\text{trace}})$ .

Since the determinant of a block matrix is  $\det \left( \begin{bmatrix} A & B \\ C & D \end{bmatrix} \right) = \det(A - BD^{-1}C)$ , we get with  $D = 1$ :  $\det(f(\mu, \Sigma)) = \det(\Sigma + \mu\mu^\top - \mu\mu^\top) = \det(\Sigma)$ .

Let  $\bar{P}_1 = f(\mu_1, \Sigma_1)$  and  $\bar{P}_2 = f(\mu_2, \Sigma_2)$ . Checking  $D_{\text{KL}}[p_{\mu_1, \Sigma_1} : p_{\mu_2, \Sigma_2}] = D_{\text{KL}}[q_{\bar{P}_1} : q_{\bar{P}_2}]$  where  $q_{\bar{P}} = p_{0, \bar{P}}$  amounts to verify that  $\text{tr}(\bar{P}_2^{-1}\bar{P}_1) = 1 + \text{tr}(\Sigma_2^{-1}\Sigma_1 + \Delta_\mu^\top \Sigma_2^{-1} \Delta_\mu)$ . Indeed, using the inverse matrix

$$f(\mu, \Sigma)^{-1} = \begin{bmatrix} \Sigma^{-1} & -\Sigma^{-1}\mu \\ -\mu^\top \Sigma^{-1} & 1 + \mu^\top \Sigma^{-1}\mu \end{bmatrix},$$

we have  $\text{tr}(\bar{P}_2^{-1}\bar{P}_1) = \text{tr} \left( \begin{bmatrix} \Sigma_2^{-1} & -\Sigma_2^{-1}\mu_2 \\ -\mu_2^\top \Sigma_2^{-1} & 1 + \mu_2^\top \Sigma_2^{-1}\mu_2 \end{bmatrix} \begin{bmatrix} \Sigma_1 + \mu_1\mu_1^\top & \mu_1 \\ \mu_1^\top & 1 \end{bmatrix} \right) = 1 + \text{tr}(\Sigma_2^{-1}\Sigma_1 + \Delta_\mu^\top \Sigma_2^{-1} \Delta_\mu)$ .

Thus even if the dimension of the sample spaces of  $p_{\mu, \Sigma}$  and  $q_{\bar{P}=f(\mu, \Sigma)}$  differs by one, we get the same KLD and Jeffreys divergence by Calvo and Oller's isometric mapping  $f$ .  $\square$

Second, the mixture geodesics are preserved by the embedding  $f$ :

**Proposition 4.5.** *The mixture geodesics are preserved by the embedding  $f$ :*

$$f(\gamma_m^{\mathcal{N}}(N_0, N_1; t)) = \gamma_m^{\mathcal{P}}(f(N_0), f(N_1); t).$$

We check that  $f(\text{LERP}(N_0, N_1; t)) = \text{LERP}(\bar{P}_0, \bar{P}_1; t)$ . Thus the pullback of the Hilbert cone geodesics are thus coinciding with the mixture geodesics on  $\mathcal{N}$ .

Therefore all algorithms on  $\mathcal{N}$  which only require  $m$ -geodesics or  $m$ -projections [5] by minimizing the right-hand side of the KLD can be implemented by algorithms on  $\mathcal{P}$  by using the  $f$ -embedding. On  $\mathcal{P}$ , the minimizing problems amounts to a logdet minimization problem well-studied in the both optimization community and information geometry community information projections [73].

However, the exponential geodesics are preserved only for submanifolds  $\mathcal{N}_\mu$  of  $\mathcal{N}$  with fixed mean  $\mu$ . Thus  $\bar{\mathcal{N}}_\mu$  preserve both mixture and exponential geodesics: The submanifolds  $\bar{\mathcal{N}}_\mu$  are said to be *doubly auto-parallel* [60].

Instead of considering the minimax center (i.e., circumcenter), we can also compute iteratively the Riemannian SPD Fréchet mean of a finite set of  $n$  SPD matrices  $S_1, \dots, S_n$ :

#### RIESTOCENTROID:

First, we let  $C_1 = S_{f_1}$  where  $f_1$  is chosen uniformly randomly in  $\{1, \dots, n\}$ . Then we iteratively update  $C_i = C_{i-1} \#_{\frac{1}{i}} S_{f_i}$  for  $i > 1$ , where  $f_i$  is chosen uniformly randomly in  $\{1, \dots, n\}$ . Convergence in probability is reported for non-positive curvature spaces in [25], and more generally for length spaces in [70]. The SPD cone is NPC but not the normal manifold which has some positive sectional curvatures [67]. To approximate the Riemannian Fisher normal centroid of  $n$  MVNs  $N(\mu_1, \Sigma_1), \dots, N(\mu_n, \Sigma_n)$ , we lift them onto the higher-dimensional SPD cone:  $\bar{N}_i = f(N(\mu_i, \Sigma_i))$ . We then apply the RIESTOCENTROID algorithm for  $T$  iterations, and pullback  $C_T$ :  $\tilde{N} = f^{-1}(C_T)$ . See Figure 10 for some illustrations.

Online materials are available at <https://franknielsen.github.io/FisherRaoMVN/>

## References

- [1] P-A Absil, Robert Mahony, and Rodolphe Sepulchre. *Optimization algorithms on matrix manifolds*. Princeton University Press, 2008.
- [2] Layth M Alabdulsada and László Kozma. On non-positive curvature properties of the hilbert metric. *The Journal of Geometric Analysis*, 29:569–576, 2019.
- [3] Syed Mumtaz Ali and Samuel D Silvey. A general class of coefficients of divergence of one distribution from another. *Journal of the Royal Statistical Society: Series B (Methodological)*, 28(1):131–142, 1966.

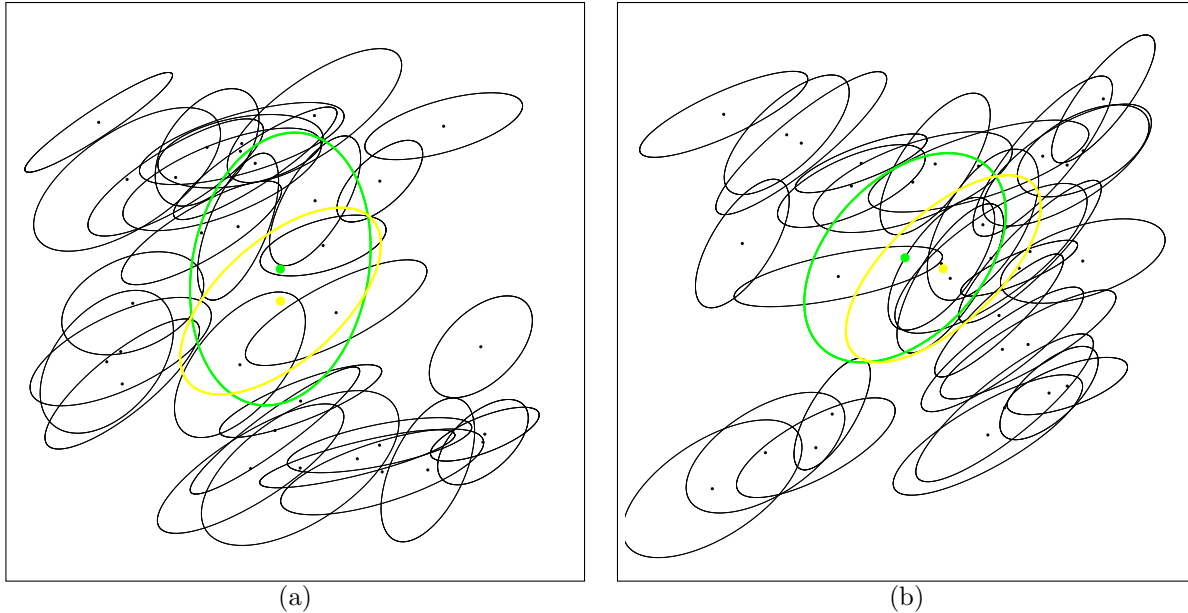


Figure 10: Approximate Fisher centroid of  $n$  bivariate normals (yellow) vs approximate Hilbert minimax center (green).

- [4] Josh Alman and Virginia Vassilevska Williams. A refined laser method and faster matrix multiplication. In *Proceedings of the 2021 ACM-SIAM Symposium on Discrete Algorithms (SODA)*, pages 522–539. SIAM, 2021.
- [5] Shun-ichi Amari. *Information Geometry and Its Applications*. Applied Mathematical Sciences. Springer Japan, 2016.
- [6] Alexandr Andoni. *Nearest neighbor search: The old, the new, and the impossible*. PhD thesis, Massachusetts Institute of Technology, 2009.
- [7] Marc Arnaudon and Frank Nielsen. On approximating the Riemannian 1-center. *Computational Geometry*, 46(1):93–104, 2013.
- [8] Giacomo Baggio, Augusto Ferrante, and Rodolphe Sepulchre. Conal distances between rational spectral densities. *IEEE Transactions on Automatic Control*, 64(5):1848–1857, 2018.
- [9] Grey Ballard, Tamara Kolda, and Todd Plantenga. Efficiently computing tensor eigenvalues on a GPU. In *2011 IEEE International Symposium on Parallel and Distributed Processing Workshops and Phd Forum*, pages 1340–1348. IEEE, 2011.
- [10] Alexandre Barachant, Stéphane Bonnet, Marco Congedo, and Christian Jutten. Multiclass brain-computer interface classification by Riemannian geometry. *IEEE Transactions on Biomedical Engineering*, 59(4):920–928, 2011.
- [11] Frédéric Barbaresco. Information geometry of covariance matrix: Cartan-Siegel homogeneous bounded domains, Mostow/Berger fibration and Fréchet median. In *Matrix information geometry*, pages 199–255. Springer, 2013.
- [12] Nitin Bhatia et al. Survey of nearest neighbor techniques. *arXiv preprint arXiv:1007.0085*, 2010.
- [13] Rajendra Bhatia. Positive definite matrices. In *Positive Definite Matrices*. Princeton university press, 2009.

- [14] Rajendra Bhatia and John Holbrook. Noncommutative geometric means. *Math. Intelligencer*, 28(1):32–39, 2006.
- [15] Garrett Birkhoff. Extensions of Jentzsch’s theorem. *Transactions of the American Mathematical Society*, 85(1):219–227, 1957.
- [16] Martin R Bridson and André Haefliger. *Metric spaces of non-positive curvature*, volume 319. Springer Science & Business Media, 2013.
- [17] Jacob Burbea and C Radhakrishna Rao. Entropy differential metric, distance and divergence measures in probability spaces: A unified approach. *Journal of Multivariate Analysis*, 12(4):575–596, 1982.
- [18] Yann Cabanes and Frank Nielsen. Classification in the Siegel Space for Vectorial Autoregressive Data. In *5th International Conference on Geometric Science of Information (GSI)*, pages 693–700. Springer, 2021.
- [19] Ovidiu Calin and Constantin Udriște. *Geometric modeling in probability and statistics*, volume 121. Springer, 2014.
- [20] Miquel Calvo and Josep M Oller. A distance between multivariate normal distributions based in an embedding into the Siegel group. *Journal of multivariate analysis*, 35(2):223–242, 1990.
- [21] Miquel Calvo and Josep Maria Oller. An explicit solution of information geodesic equations for the multivariate normal model. *Statistics & Risk Modeling*, 9(1-2):119–138, 1991.
- [22] Chad Carson, Serge Belongie, Hayit Greenspan, and Jitendra Malik. Blobworld: Image segmentation using expectation-maximization and its application to image querying. *IEEE Transactions on pattern analysis and machine intelligence*, 24(8):1026–1038, 2002.
- [23] Zeineb Chebbi and Maher Moakher. Means of Hermitian positive-definite matrices based on the log-determinant  $\alpha$ -divergence function. *Linear Algebra and its Applications*, 436(7):1872–1889, 2012.
- [24] Yongxin Chen, Tryphon T Georgiou, and Michele Pavon. Stochastic control liaisons: Richard Sinkhorn meets Gaspard Monge on a Schrodinger bridge. *Siam Review*, 63(2):249–313, 2021.
- [25] Guang Cheng, Jeffrey Ho, Hesamoddin Salehian, and Baba C Vemuri. Recursive computation of the Fréchet mean on non-positively curved Riemannian manifolds with applications. *Riemannian Computing in Computer Vision*, pages 21–43, 2016.
- [26] Thomas H Cormen, Charles E Leiserson, Ronald L Rivest, and Clifford Stein. *Introduction to algorithms*. MIT press, 2022.
- [27] Imre Csiszár. Information-type measures of difference of probability distributions and indirect observation. *studia scientiarum Mathematicarum Hungarica*, 2:229–318, 1967.
- [28] Jason Davis and Inderjit Dhillon. Differential entropic clustering of multivariate Gaussians. *Advances in Neural Information Processing Systems*, 19, 2006.
- [29] Alberto Dolcetti and Donato Pertici. Elliptic isometries of the manifold of positive definite real matrices with the trace metric. *Rendiconti del Circolo Matematico di Palermo Series 2*, 70(1):575–592, 2021.
- [30] Delbert Dueck and Brendan J Frey. Non-metric affinity propagation for unsupervised image categorization. In *2007 IEEE 11th International Conference on Computer Vision*, pages 1–8. IEEE, 2007.
- [31] Poul Svante Eriksen. Geodesics connected with the Fisher metric on the multivariate normal manifold. Technical Report 86-13, Institute of Electronic Systems, Aalborg University Centre, Denmark, 1986.

- [32] PS Eriksen. Geodesics connected with the Fisher metric on the multivariate normal manifold. In *Proceedings of the GST Workshop, Lancaster, UK*, pages 28–31, 1987.
- [33] Shmuel Friedland and Pedro J Freitas. Revisiting the Siegel upper half plane I. *Linear algebra and its applications*, 376:19–44, 2004.
- [34] Hitoshi Furuhashi, Jun-ichi Inoguchi, and Shimpei Kobayashi. A characterization of the alpha-connections on the statistical manifold of normal distributions. *Information Geometry*, 4(1):177–188, 2021.
- [35] Yansong Gao and Pratik Chaudhari. An information-geometric distance on the space of tasks. In *International Conference on Machine Learning*, pages 3553–3563. PMLR, 2021.
- [36] Leonor Godinho and José Natário. An introduction to Riemannian geometry. *With Applications*, 2012.
- [37] Jacob Goldberger, Hayit K Greenspan, and Jeremie Dreyfuss. Simplifying mixture models using the unscented transform. *IEEE Transactions on Pattern Analysis and Machine Intelligence*, 30(8):1496–1502, 2008.
- [38] Teofilo F Gonzalez. Clustering to minimize the maximum intercluster distance. *Theoretical computer science*, 38:293–306, 1985.
- [39] Roger B Grosse, Chris J Maddison, and Russ R Salakhutdinov. Annealing between distributions by averaging moments. *Advances in Neural Information Processing Systems*, 26, 2013.
- [40] Minyeon Han and Frank C Park. DTI segmentation and fiber tracking using metrics on multivariate normal distributions. *Journal of mathematical imaging and vision*, 49:317–334, 2014.
- [41] Alfred O Hero, Bing Ma, Olivier Michel, and John Gorman. Alpha-divergence for classification, indexing and retrieval. *Communication and Signal Processing Laboratory, Technical Report CSPL-328, U. Mich*, 2001.
- [42] David Hilbert. Über die Gerade Linie als Kurzeste Verbindung Zweier Punkte. *Mathematische Annalen*, 46(1):91–96, 1895.
- [43] Reshad Hosseini and Suvrit Sra. Matrix manifold optimization for Gaussian mixtures. *Advances in Neural Information Processing Systems*, 28, 2015.
- [44] Harold Hotelling. Spaces of statistical parameters. *Bull. Amer. Math. Soc*, 36:191, 1930.
- [45] Takuro Imai, Akira Takaesu, and Masato Wakayama. Remarks on geodesics for multivariate normal models. Technical report, Faculty of Mathematics, Kyushu University, 2011.
- [46] A. T. James. The variance information manifold and the functions on it. In *Multivariate Analysis—III*, pages 157–169. Elsevier, 1973.
- [47] Anders Karlsson and Guennadi A Noskov. *The Hilbert metric and Gromov hyperbolicity*. Sonderforschungsbereich 343, 2000.
- [48] Leonard Kaufman. Partitioning around medoids (program PAM). *Finding groups in data*, 344:68–125, 1990.
- [49] Shimpei Kobayashi. Geodesics of multivariate normal distributions and a Toda lattice type Lax pair. *arXiv preprint arXiv:2304.12575*, 2023.
- [50] Elon Kohlberg and John W Pratt. The contraction mapping approach to the Perron-Frobenius theory: Why Hilbert’s metric? *Mathematics of Operations Research*, 7(2):198–210, 1982.

- [51] Junghyun Kwon, Kyoung Mu Lee, and Frank C Park. Visual tracking via geometric particle filtering on the affine group with optimal importance functions. In *2009 IEEE Conference on Computer Vision and Pattern Recognition*, pages 991–998. IEEE, 2009.
- [52] Serge Lang and Serge Lang. Bruhat-Tits spaces. *Math Talks for Undergraduates*, pages 79–100, 1999.
- [53] Stuart Lloyd. Least squares quantization in PCM. *IEEE transactions on information theory*, 28(2):129–137, 1982.
- [54] Maher Moakher. A differential geometric approach to the geometric mean of symmetric positive-definite matrices. *SIAM journal on matrix analysis and applications*, 26(3):735–747, 2005.
- [55] Yoshimasa Nakamura. Algorithms associated with arithmetic, geometric and harmonic means and integrable systems. *Journal of computational and applied mathematics*, 131(1-2):161–174, 2001.
- [56] Frank Nielsen. A Simple Approximation Method for the Fisher–Rao Distance between Multivariate Normal Distributions. *Entropy*, 25(4):654, 2023.
- [57] Frank Nielsen and Gaëtan Hadjeres. Monte Carlo information-geometric structures. *Geometric Structures of Information*, pages 69–103, 2019.
- [58] Frank Nielsen, Paolo Piro, and Michel Barlaud. Bregman vantage point trees for efficient nearest neighbor queries. In *2009 IEEE International Conference on Multimedia and Expo*, pages 878–881. IEEE, 2009.
- [59] Roger D Nussbaum. Finsler structures for the part metric and Hilbert’s projective metric and applications to ordinary differential equations. *Differential and Integral Equations*, 7(6):1649–1707, 1994.
- [60] Atsumi Ohara. Doubly autoparallel structure on positive definite matrices and its applications. In *International Conference on Geometric Science of Information*, pages 251–260. Springer, 2019.
- [61] Marion Pilté and Frédéric Barbaresco. Tracking quality monitoring based on information geometry and geodesic shooting. In *2016 17th International Radar Symposium (IRS)*, pages 1–6. IEEE, 2016.
- [62] Julianna Pinele, João E Strapasson, and Sueli I R Costa. The Fisher–Rao distance between multivariate normal distributions: Special cases, bounds and applications. *Entropy*, 22(4):404, 2020.
- [63] Fatih Porikli, Oncel Tuzel, and Peter Meer. Covariance tracking using model update based on Lie algebra. In *2006 IEEE Computer Society Conference on Computer Vision and Pattern Recognition (CVPR’06)*, volume 1, pages 728–735. IEEE, 2006.
- [64] C R Rao. Information and accuracy attainable in the estimation of statistical parameters. *Bulletin of the Calcutta Mathematical Society*, 37(3):81–91, 1945.
- [65] Yao Rong, Mengjiao Tang, and Jie Zhou. Intrinsic losses based on information geometry and their applications. *Entropy*, 19(8):405, 2017.
- [66] Carl Ludwig Siegel. *Symplectic geometry*. Academic Press, 1964.
- [67] Lene Theil Skovgaard. A Riemannian geometry of the multivariate normal model. *Scandinavian journal of statistics*, pages 211–223, 1984.
- [68] Suvrit Sra. Positive definite matrices and the  $S$ -divergence. *Proceedings of the American Mathematical Society*, 144(7):2787–2797, 2016.
- [69] João E Strapasson, Julianna Pinele, and Sueli IR Costa. Clustering using the Fisher-Rao distance. In *2016 IEEE Sensor Array and Multichannel Signal Processing Workshop (SAM)*, pages 1–5. IEEE, 2016.

- [70] Karl-Theodor Sturm. Probability measures on metric spaces of nonpositive. *Heat Kernels and Analysis on Manifolds, Graphs, and Metric Spaces: Lecture Notes from a Quarter Program on Heat Kernels, Random Walks, and Analysis on Manifolds and Graphs: April 16-July 13, 2002, Emile Borel Centre of the Henri Poincaré Institute, Paris, France*, 338:357, 2003.
- [71] Asuka Takatsu. Wasserstein geometry of Gaussian measures. *Osaka Journal of Mathematics*, 48(4):1005 – 1026, 2011.
- [72] Luca Trevisan. Lecture notes on graph partitioning, expanders and spectral methods. *University of California, Berkeley*, 2017.
- [73] Koji Tsuda, Shotaro Akaho, and Kiyoshi Asai. The em algorithm for kernel matrix completion with auxiliary data. *The Journal of Machine Learning Research*, 4:67–81, 2003.
- [74] Oncel Tuzel, Fatih Porikli, and Peter Meer. Pedestrian detection via classification on Riemannian manifolds. *IEEE transactions on pattern analysis and machine intelligence*, 30(10):1713–1727, 2008.
- [75] Emo Welzl. Smallest enclosing disks (balls and ellipsoids). In *New Results and New Trends in Computer Science*, pages 359–370. Springer, 2005.
- [76] Peter N Yianilos. Data structures and algorithms for nearest neighbor. In *Proceedings of the ACM-SIAM Symposium on Discrete algorithms*, volume 66, page 311, 1993.
- [77] Shintaro Yoshizawa and Kunio Tanabe. Dual differential geometry associated with the Kullback-Leibler information on the Gaussian distributions and its 2-parameter deformations. *SUT Journal of Mathematics*, 35(1):113–137, 1999.
- [78] Tadashi Yoshizawa. A geometry of parameter space and its statistical interpretation. *Kokyuroku*, pages 103–131, 1972.
- [79] Kai Zhang and James T Kwok. Simplifying mixture models through function approximation. *IEEE Transactions on Neural Networks*, 21(4):644–658, 2010.

## A Fisher-Rao geodesics between MVNs with initial value conditions

The Fisher-Rao geodesics  $\gamma(t)$  are smooth curves which are autoparallel with respect to the Levi-Civita connection  $\nabla^g$  induced by the metric tensor  $g$ :  $\nabla_{\dot{\gamma}}^g \dot{\gamma} = 0$ . On the MVN manifold, the system of Riemannian geodesic equations [67] is

$$\begin{cases} \ddot{\mu} - \dot{\Sigma} \Sigma^{-1} \dot{\mu} & = 0, \\ \ddot{\Sigma} + \dot{\mu} \dot{\mu}^\top - \dot{\Sigma} \Sigma^{-1} \dot{\Sigma} & = 0. \end{cases}$$

We may solve the above differential equation system either using initial value conditions (IVPs) by prescribing  $N_0 = (\mu(0), \Sigma(0))$  and a tangent vector  $\dot{N}(0) = (\dot{\mu}(0), \dot{\Sigma}(0))$ , or with boundary value conditions (BVPs) by prescribing  $N_0 = (\mu(0), \Sigma(0))$  and  $N_1 = (\mu(1), \Sigma(1))$ . Let  $\gamma_{\mathcal{N}}^{\text{Fisher}}(N_0, \dot{N}_0; t)$  and  $\gamma_{\mathcal{N}}^{\text{Fisher}}(N_0, N_1; t)$  denote these two types of geodesics.

Without loss of generality, let us assume  $N_0 = N(0, I)$  (standard normal distribution). The task is to perform geodesic shooting, i.e., calculate  $N(t) = \gamma_{\mathcal{N}}^{\text{Fisher}}(N_0, v_0; t)$  with some prescribed initial condition  $(v, S) = \dot{\gamma}_{\mathcal{N}}^{\text{Fisher}}(N_0, v_0; 0) \in T_{N_{\text{std}}} \mathcal{M}$  and  $t \geq 0$ .

## A.1 Eriksen's homogeneous symmetric space solution

We use the following natural parameterization of the normal distributions:

$$(\xi = \Sigma^{-1}\mu, \Xi = \Sigma^{-1}).$$

The initial conditions are given by  $(a = \dot{\xi}(0), B = \dot{\Xi}(0)) = \dot{\gamma}_{\mathcal{N}}^{\text{Fisher}}(N_{\text{std}}, v_0; 0)$  at the standard normal distribution  $N_{\text{std}}$ . Eriksen's method proceeds as follows to calculate  $\underline{\gamma}_{\text{FR}}^{\mathcal{N}}(N_{\text{std}}, v_0; t)$ :

- Build a  $(2d + 1) \times (2d + 1)$  matrix  $A$ :

$$A = \begin{bmatrix} -B & a & 0 \\ a^\top & 0 & -a^\top \\ 0 & -a & B \end{bmatrix}.$$

- Compute matrix  $M(t) = \exp(tA)$  for the prescribed value  $t > 0$ . To calculate  $\exp(M)$ , we first compute the eigen decomposition of  $AM = O \text{diag}(\lambda_1, \dots, \lambda_d) O^\top$  and then reports  $O \text{diag}(\exp(\lambda_1), \dots, \exp(\lambda_d)) O^\top$ .
- Extract  $(\xi(t), \Xi(t))$  from  $M(t)$  and convert to  $(\mu(t), \Sigma(t))$ :

$$\begin{aligned} \Sigma(t) &= [M(t)]_{1:d, 1:d}^{-1}, \\ \mu(t) &= \Sigma(t)[M(t)]_{1:d, d+1}. \end{aligned}$$

- Report  $\underline{\gamma}_{\text{FR}}^{\mathcal{N}}(N_{\text{std}}, v_0; t) = (\mu(t), \Sigma(t))$ .

Eriksen's method yields a pregeodesic and not a geodesic. For geodesics, we have the following Fisher-Rao distance property  $\rho_{\mathcal{N}}(\gamma_{\text{FR}}^{\mathcal{N}}(N_{\text{std}}, v_0; s), \gamma_{\text{FR}}^{\mathcal{N}}(N_{\text{std}}, v_0; t)) = |s - t| \rho_{\mathcal{N}}(\gamma_{\text{FR}}^{\mathcal{N}}(N_0, N_1))$  where  $N_0 = N_{\text{std}}$  and  $N_1 = \gamma_{\text{FR}}^{\mathcal{N}}(N_{\text{std}}, v_0; 1)$ .

## A.2 Calvo and Oller's direction solution

We report the solution given in [21] which relies on the following natural parameterization of the normal distributions

$$(\xi = \Sigma^{-1}\mu, \Xi = \Sigma^{-1}).$$

The initial conditions are given by  $(a = \dot{\xi}(0), B = \dot{\Xi}(0)) = \dot{\gamma}_{\mathcal{N}}^{\text{Fisher}}(N_0, v_0; 0)$ .

The method of [21] first calculate those quantities:

$$\begin{aligned} B &= -\Xi(0)^{-\frac{1}{2}} \dot{\Xi}(0) \Xi(0)^{-\frac{1}{2}}, \\ a &= \Xi(0)^{-\frac{1}{2}} \dot{\xi}(0) + B \Xi(0)^{-\frac{1}{2}} \xi(0), \\ G &= (B^2 + 2aa^\top)^{\frac{1}{2}}. \end{aligned}$$

Furthermore, let  $G^\dagger = G^{-1}$  when  $G$  is invertible or  $G^\dagger = (G^\top G)^{-1} G^\top$  the Moore-Penrose generalized pseudo-inverse matrix of  $G$  otherwise (or any kind of generalized matrix inverse  $G^-$  [21], see).

Then we have  $(\xi(t), \Xi(t)) = \gamma_{\mathcal{N}}^{\text{Fisher}}(N_0, v_0; t)$  with

$$\begin{aligned} \Xi(t) &= \Xi(0)^{\frac{1}{2}} R(t) R(t)^\top \Xi(0)^{\frac{1}{2}}, \\ \xi(t) &= 2\Xi(0)^{\frac{1}{2}} R(t) \text{Sinh}\left(\frac{1}{2} Gt\right) G^\dagger a + \Xi(t) \Xi^{-1}(0) \xi(0), \end{aligned}$$

and

$$R(t) = \text{Cosh}\left(\frac{1}{2} Gt\right) - B G^\dagger \text{Sinh}\left(\frac{1}{2} Gt\right).$$



The matrix hyperbolic cosine and sinus functions of  $M$  are calculated from the eigen decomposition of  $M = O \text{diag}(\lambda_1, \dots, \lambda_d) O^\top$  as follows:

$$\begin{aligned} \text{Sinh}(M) &= O \text{diag}(\sinh(\lambda_1), \dots, \sinh(\lambda_d)) O^\top, & \sinh(u) &= \frac{e^u - e^{-u}}{2} = \sum_{i=0}^{\infty} \frac{u^{2i+1}}{(2i+1)!}, \\ \text{Cosh}(M) &= O \text{diag}(\cosh(\lambda_1), \dots, \cosh(\lambda_d)) O^\top, & \cosh(u) &= \frac{e^u + e^{-u}}{2} = \sum_{i=0}^{\infty} \frac{u^{2i}}{(2i)!}. \end{aligned}$$

For the general case  $\gamma_{\mathcal{N}}^{\text{Fisher}}(N, v_0; t)$  with arbitrary  $N = (\Sigma, \mu)$ , we use the affine equivariance property of the Fisher-Rao geodesics with  $P = \Sigma^{-\frac{1}{2}}$ :

$$\gamma_{\mathcal{N}}^{\text{Fisher}}(N, v_0; t) = (-P\mu, P^{-1}) \cdot \gamma_{\mathcal{N}}^{\text{Fisher}}(N_{\text{std}}, (Pa, -PBP^\top); t). \quad (19)$$

Figure 11 displays several examples of geodesics from the standard normal distribution with various initial value conditions.

The geodesics with initial values let us define the Riemannian exponential map  $\exp : T_N \mathcal{M} \rightarrow \mathcal{M}$ :

$$\exp_N(v) = \gamma_{\mathcal{N}}^{\text{Fisher}}(N, v; 1).$$

The inverse map is the Riemannian logarithm map. In a geodesically complete manifold (e.g.,  $\mathcal{N}_\mu$ ), we can express the Fisher-Rao distance as:

$$\rho_{\mathcal{N}}(N_1, N_2) = \|\text{Log}_{N_1}(N_2)\|_{N_1}.$$

Thus computing the Fisher-Rao distance can be done by computing the Riemannian MVN logarithm.

## B Proof of square root of Jeffreys upper bound

Let us prove that the Fisher-Rao distance between normal distributions is upper bounded by the square root of the Jeffreys divergence:

$$\rho_{\mathcal{N}}(N_1, N_2) \leq \sqrt{D_J(N_1, N_2)}.$$

*Property 2.* We have

$$D_J[p_{\lambda_1}, p_{\lambda_2}] = \int_0^1 ds_{\mathcal{N}}^2(\gamma_{\mathcal{N}}^m(p_{\lambda_1}, p_{\lambda_2}; t)) dt = \int_0^1 ds_{\mathcal{N}}^2(\gamma_{\mathcal{N}}^e(p_{\lambda_1}, p_{\lambda_2}; t)) dt.$$

Let  $S_F(\theta_1; \theta_2) = B_F(\theta_1 : \theta_2) + B_F(\theta_2 : \theta_1)$  be a symmetrized Bregman divergence. Let  $ds^2 = d\theta^\top \nabla^2 F(\theta) d\theta$  denote the squared length element on the Bregman manifold and denote by  $\gamma(t)$  and  $\gamma^*(t)$  the dual geodesics connecting  $\theta_1$  to  $\theta_2$ . We can express  $S_F(\theta_1; \theta_2)$  as integral energies on dual geodesics:

*Property 3.* We have  $S_F(\theta_1; \theta_2) = \int_0^1 ds^2(\gamma(t)) dt = \int_0^1 ds^2(\gamma^*(t)) dt$ .

*Proof.* The proof that the symmetrized Bregman divergence amount to these energy integrals is based on the first-order and second-order directional derivatives. The first-order directional derivative  $\nabla_u F(\theta)$  with respect to vector  $u$  is defined by

$$\nabla_u F(\theta) = \lim_{t \rightarrow 0} \frac{F(\theta + tv) - F(\theta)}{t} = v^\top \nabla F(\theta).$$

The second-order directional derivatives  $\nabla_{u,v}^2 F(\theta)$  is

$$\begin{aligned} \nabla_{u,v}^2 F(\theta) &= \nabla_u \nabla_v F(\theta), \\ &= \lim_{t \rightarrow 0} \frac{v^\top \nabla F(\theta + tu) - v^\top \nabla F(\theta)}{t}, \\ &= u^\top \nabla^2 F(\theta) v. \end{aligned}$$

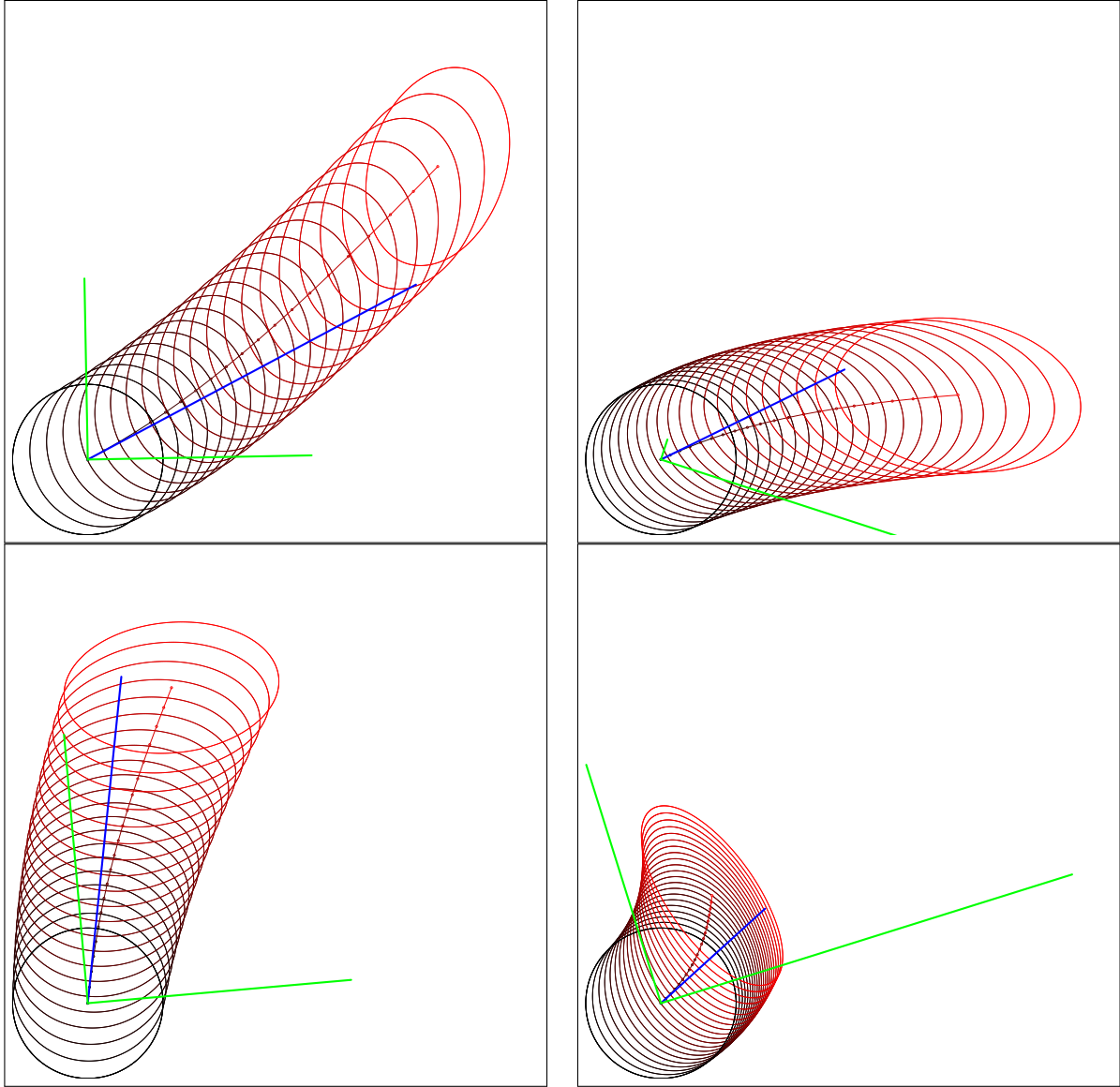


Figure 11: Examples of Fisher-Rao geodesics  $(\mu(t), \Sigma(t))$  emanating from the standard bivariate normal distribution  $(\mu(0), \Sigma(0)) = N(0, I)$  with initial value conditions  $(\dot{\mu}(0), \dot{\Sigma}(0))$ . Vectors  $\mu(0)$  are shown in blue and symmetric matrices  $\dot{\Sigma}(0) = \lambda_1 v_1 v_1^\top + \lambda_2 v_2 v_2^\top$  are visualized by their two scaled eigenvectors  $\lambda_1 v_1$  and  $\lambda_2 v_2$  shown in green.

Now consider the squared length element  $ds^2(\gamma(t))$  on the primal geodesic  $\gamma(t)$  expressed using the primal coordinate system  $\theta$ :  $ds^2(\gamma(t)) = d\theta(t)^\top \nabla^2 F(\theta(t)) d\theta(t)$  with  $\theta(\gamma(t)) = \theta_1 + t(\theta_2 - \theta_1)$  and  $d\theta(t) = \theta_2 - \theta_1$ . Let us express the  $ds^2(\gamma(t))$  using the second-order directional derivative:

$$ds^2(\gamma(t)) = \nabla_{\theta_2 - \theta_1}^2 F(\theta(t)).$$

Thus we have  $\int_0^1 ds^2(\gamma(t)) dt = [\nabla_{\theta_2 - \theta_1} F(\theta(t))]_0^1$ , where the first-order directional derivative is  $\nabla_{\theta_2 - \theta_1} F(\theta(t)) = (\theta_2 - \theta_1)^\top \nabla F(\theta(t))$ . Therefore we get  $\int_0^1 ds^2(\gamma(t)) dt = (\theta_2 - \theta_1)^\top (\nabla F(\theta_2) - \nabla F(\theta_1)) = S_F(\theta_1; \theta_2)$ .

Similarly, we express the squared length element  $ds^2(\gamma^*(t))$  using the dual coordinate system  $\eta$  as the second-order directional derivative of  $F^*(\eta(t))$  with  $\eta(\gamma^*(t)) = \eta_1 + t(\eta_2 - \eta_1)$ :

$$ds^2(\gamma^*(t)) = \nabla_{\eta_2 - \eta_1}^2 F^*(\eta(t)).$$

Therefore, we have  $\int_0^1 ds^2(\gamma^*(t)) dt = [\nabla_{\eta_2 - \eta_1} F^*(\eta(t))]_0^1 = S_{F^*}(\eta_1; \eta_2)$ . Since  $S_{F^*}(\eta_1; \eta_2) = S_F(\theta_1; \theta_2)$ , we conclude that

$$S_F(\theta_1; \theta_2) = \int_0^1 ds^2(\gamma(t)) dt = \int_0^1 ds^2(\gamma^*(t)) dt$$

Note that in 1D, both pregeodesics  $\gamma(t)$  and  $\gamma^*(t)$  coincide. We have  $ds^2(t) = (\theta_2 - \theta_1)^2 f''(\theta(t)) = (\eta_2 - \eta_1) f^{*''}(\eta(t))$  so that we check that  $S_F(\theta_1; \theta_2) = \int_0^1 ds^2(\gamma(t)) dt = (\theta_2 - \theta_1) [f'(\theta(t))]_0^1 = (\eta_2 - \eta_1) [f^{*'}(\eta(t))]_0^1 = (\eta_2 - \eta_1)(\theta_2 - \theta_1)$ .  $\square$

*Property 4* ([5]). We have

$$D_J[p_{\lambda_1}, p_{\lambda_2}] = \int_0^1 ds_{\mathcal{N}}^2(\gamma_{\mathcal{N}}^m(p_{\lambda_1}, p_{\lambda_2}; t)) dt = \int_0^1 ds_{\mathcal{N}}^2(\gamma_{\mathcal{N}}^e(p_{\lambda_1}, p_{\lambda_2}; t)) dt.$$

*Proof.* Let us report a proof of this remarkable fact in the general setting of Bregman manifolds. Indeed, since

$$D_J[p_{\lambda_1}, p_{\lambda_2}] = D_{\text{KL}}[p_{\lambda_1} : p_{\lambda_2}] + D_{\text{KL}}[p_{\lambda_2} : p_{\lambda_1}],$$

and  $D_{\text{KL}}[p_{\lambda_1} : p_{\lambda_2}] = B_F(\theta(\lambda_2) : \theta(\lambda_1))$ , where  $B_F$  denotes the Bregman divergence induced by the cumulant function of the multivariate normals and  $\theta(\lambda)$  is the natural parameter corresponding to  $\lambda$ , we have

$$\begin{aligned} D_J[p_{\lambda_1}, p_{\lambda_2}] &= B_F(\theta_1 : \theta_2) + B_F(\theta_2 : \theta_1), \\ &= S_F(\theta_1; \theta_2) = (\theta_2 - \theta_1)^\top (\eta_2 - \eta_1) = S_{F^*}(\eta_1; \eta_2), \end{aligned}$$

where  $\eta = \nabla F(\theta)$  and  $\theta = \nabla F^*(\eta)$  denote the dual parameterizations obtained by the Legendre-Fenchel convex conjugate  $F^*(\eta)$  of  $F(\theta)$ . Moreover, we have  $F^*(\eta) = -h(p_{\mu, \Sigma})$  [5], i.e., the convex conjugate function is Shannon negentropy.

Then we conclude by using the fact that  $S_F(\theta_1; \theta_2) = \int_0^1 ds^2(\gamma(t)) dt = \int_0^1 ds^2(\gamma^*(t)) dt$ , i.e., the symmetrized Bregman divergence amounts to integral energies on dual geodesics on a Bregman manifold. The proof of this general property is reported in Appendix B.  $\square$

*Property 5* (Fisher–Rao upper bound). The Fisher–Rao distance between normal distributions is upper bounded by the square root of the Jeffreys divergence:  $\rho_{\mathcal{N}}(N_1, N_2) \leq \sqrt{D_J(N_1, N_2)}$ .

*Proof.* Consider the Cauchy-Schwarz inequality for positive functions  $f(t)$  and  $g(t)$ :

$$\int_0^1 f(t) g(t) dt \leq \sqrt{\left( \int_0^1 f(t)^2 dt \right) \left( \int_0^1 g(t)^2 dt \right)},$$

and let  $f(t) = ds_{\mathcal{N}}(\gamma_{\mathcal{N}}^c(p_{\lambda_1}, p_{\lambda_2}; t))$  and  $g(t) = 1$ . Then we get:

$$\left( \int_0^1 ds_{\mathcal{N}}(\gamma_{\mathcal{N}}^c(p_{\lambda_1}, p_{\lambda_2}; t)) dt \right)^2 \leq \left( \int_0^1 ds_{\mathcal{N}}^2(\gamma_{\mathcal{N}}^c(p_{\lambda_1}, p_{\lambda_2}; t)) dt \right) \left( \underbrace{\int_0^1 1^2 dt}_{=1} \right).$$

Furthermore since by definition of  $\gamma_{\mathcal{N}}^{\text{FR}}$ , we have

$$\int_0^1 ds_{\mathcal{N}}(\gamma_{\mathcal{N}}^c(p_{\lambda_1}, p_{\lambda_2}; t)) dt \geq \int_0^1 ds_{\mathcal{N}}(\gamma_{\mathcal{N}}^{\text{FR}}(p_{\lambda_1}, p_{\lambda_2}; t)) dt =: \rho_{\mathcal{N}}(N_1, N_2).$$

It follows for  $c = \gamma_{\mathcal{N}}^e$  (i.e.,  $e$ -geodesic) using Property 4 that we have:

$$\rho_{\mathcal{N}}(N_1, N_2)^2 \leq \int_0^1 ds_{\mathcal{N}}^2(\gamma_{\mathcal{N}}^e(p_{\lambda_1}, p_{\lambda_2}; t)) dt = D_J(N_1, N_2).$$

Thus we conclude that  $\rho_{\mathcal{N}}(N_1, N_2) \leq \sqrt{D_J(N_1, N_2)}$ .

Note that in Riemannian geometry, a curve  $\gamma$  minimizes the energy  $E(\gamma) = \int_0^1 \|\dot{\gamma}(t)\|^2 dt$  if it minimizes the length  $\text{Len}(\gamma) = \int_0^1 \|\dot{\gamma}(t)\| dt$  and  $\|\dot{\gamma}(t)\|$  is constant. Using Cauchy-Schwartz inequality, we can show that  $\text{Len}(\gamma) \leq E(\gamma)$ .  $\square$

## C Riemannian SPD geodesic and the arithmetic-harmonic inductive mean

The Riemannian SPD geodesic  $\gamma(X, Y; t)$  joining two SPD matrices  $X$  and  $Y$  with respect to the trace metric can be expressed using the weighted matrix geometric mean:

$$\gamma(X, Y; t) = X \#_t Y = X^{\frac{1}{2}} \left( X^{-\frac{1}{2}} Y X^{-\frac{1}{2}} \right)^t X^{\frac{1}{2}}. \quad (20)$$

We denote by  $X \# Y = X \#_{\frac{1}{2}} Y$ . For  $t \in (0, 1)$ ,  $X \#_t Y$  defines a matrix mean [14] of  $X$  and  $Y$  which is asymmetric when  $t \neq \frac{1}{2}$ .

The matrix geometric mean can be computed inductively using the following arithmetic-harmonic sequence:

$$\begin{aligned} A_{t+1} &= A(A_t, H_t), \\ H_{t+1} &= H(A_t, H_t), \end{aligned}$$

where the matrix arithmetic mean is  $A(X, Y) = \frac{X+Y}{2}$  and the matrix harmonic mean is  $H(X, Y) = 2(X^{-1} + Y^{-1})^{-1}$ . The sequence is initialized with  $A_0 = X$  and  $H_0 = Y$ . We have  $\text{AHM}(X, Y) = \lim_{t \rightarrow \infty} A_t = \lim_{t \rightarrow \infty} H_t = X \#_{\frac{1}{2}} Y$ , and the convergence is of quadratic order [55]. This iterative method converges to  $X \# Y$ , the non-weighted matrix geometric mean. In general, taking weighted arithmetic and harmonic means  $A(X, Y) = (1 - \alpha)X + \alpha Y$  and  $H(X, Y) = ((1 - \alpha)X^{-1} + \alpha Y^{-1})^{-1}$  yields convergence to a matrix which is not the weighted geometric mean  $X \#_{\alpha} Y$  (except when  $\alpha = \frac{1}{2}$ ). The method requires to compute the matrix harmonic mean which requires to inverse matrices. The closed-form formula of the matrix weighted geometric mean of Eq. 20 requires to compute a matrix fractional power which can be done from a matrix eigen decomposition.

## D Power method to approximate the largest and smallest eigenvalues

We concisely recall the power method and its computational complexity to approximate the largest eigenvalue  $\lambda_1$  of a  $d \times d$  symmetric positive-definite matrix  $P$  following [72]:

- Pick uniformly at random  $x^{(0)} \in \{-1, 1\}^d$
- For  $t \in (1, \dots, T)$  do  $x^{(t)} \leftarrow P x^{(t-1)}$
- Return  $\tilde{\lambda}_1 = \frac{\langle x^{(T)}, P x^{(T)} \rangle}{\langle x^{(T)}, x^{(T)} \rangle}$ , where  $\langle x, y \rangle = x^\top y$  denotes the dot product.

The complexity of the power method with  $T$  iterations is  $O(T(d+m))$  where  $m = O(d^2)$  is the number of non-zero entries of  $P$ . Furthermore, with probability  $\geq \frac{3}{16}$ , the iterative power method with  $T = O(\frac{d}{\epsilon})$  iterations yields  $\tilde{\lambda}_1 \geq (1 - \epsilon)\lambda_1$  for any  $\epsilon > 0$  [72]. Due to its vector-matrix product operations, the power method can be efficiently implemented on GPU [9].

To compute an approximation  $\tilde{\lambda}_d$  of the smallest eigenvalues  $\lambda_d$  of  $P$ , we first compute the matrix inverse  $P^{-1}$  and then compute the approximation of the largest eigenvalue of  $P^{-1}$ . We report  $\tilde{\lambda}_d(P) = \tilde{\lambda}_1(P^{-1})$ . The complexity of computing a matrix inverse is as hard as computing the matrix product [26]. The current best algorithm requires  $O(d^\omega)$  operations with  $\omega = 2.373$  [4].

## E Source code for Fisher-Rao normal geodesics

```
1 // (c) 2023 Frank.Nielsen@acm.org
2
3 import Jama.*;
4
5 class FisherRaoMVN
6 {
7     public static double sqr(double x) {
8         return x*x;
9     }
10
11     public static double min(double a, double b) {
12         if (a<b) return a;
13         else return b;
14     }
15     public static double max(double a, double b) {
16         if (a>b) return a;
17         else return b;
18     }
19
20     public static double arccosh(double x)
21     {
22         return Math.log(x+Math.sqrt(x*x-1.0));
23     }
24
25
26     public static Matrix InductiveAHM(Matrix X, Matrix Y, int nbiter)
27     {
28         Matrix XX,YY;
29         int i;
30
31         for(i=0;i<nbiter;i++)
```

```

32 {
33     XX=ArithmeticMean(X,Y);
34     YY=HarmonicMean(X,Y);
35     X=XX;Y=YY;
36 }
37 return X;
38 }
39
40
41 public static double MobiusDistance(double a, double b, double c, double d)
42 {
43     return Math.sqrt((sqr(c-a)+2.0*sqr(d-b))/(sqr(c-a)+2.0*sqr(d+b)));
44 }
45
46 // OK
47 public static double RaoDistance1D(double m1, double s1, double m2, double s2)
48 {
49     return Math.sqrt(2)*Math.log((1.0+MobiusDistance(m1, s1, m2, s2))/(1.0-
50         MobiusDistance(m1, s1, m2, s2)));
51 }
52 public static Matrix ArithmeticMean(Matrix X, Matrix Y)
53 {
54     return (X.times(0.5)).plus(Y.times(.05));
55 }
56
57 public static Matrix HarmonicMean(Matrix X, Matrix Y)
58 {
59     return (X.inverse().times(0.5)).plus(Y.inverse().times(0.5)).inverse();
60 }
61
62
63
64 public static Matrix IsometricSPDEmbeddingCalvoOller(vM N)
65 {
66     Matrix mu=N.v;
67     Matrix Sigma=N.M;
68     int d=mu.getRowDimension();
69     Matrix res=new Matrix(d+1, d+1);
70     Matrix tmp=new Matrix(d, d);
71
72     int i, j;
73
74     tmp=Sigma.plus( (mu.times(mu.transpose())) );
75
76 // Left top corner
77 for (i=0; i<d; i++)
78     for (j=0; j<d; j++)
79     {
80         res.set(i, j, tmp.get(i, j));
81     }
82
83 // Left column
84 for (i=0; i<d; i++)
85 {
86     res.set(d, i, mu.get(i, 0));

```

```

87     }
88
89     // Bottom row
90     for (i=0; i<d; i++)
91     {
92         res.set(i, d, mu.get(i, 0));
93     }
94
95     // Last element is one
96     res.set(d, d, 1);
97
98     return res;
99 }
100
101 public static double LowerBoundCalvoOller(vM N1, vM N2)
102 {
103     Matrix P1bar=IsometricSPDEmbeddingCalvoOller(N1);
104     Matrix P2bar=IsometricSPDEmbeddingCalvoOller(N2);
105     // We calculated (1/sqrt(2))*RiemannSPD(d+1)
106     return ScaledRiemannianSPDDistance(P1bar, P2bar);
107 }
108
109 public static double UpperBoundSqrtJeffreys(vM N1, vM N2)
110 {
111     return Math.sqrt(JeffreysMVN(N1, N2));
112 }
113
114 public static double JeffreysMVN(vM N1, vM N2)
115 {
116     return KLMVN(N1.v, N1.M, N2.v, N2.M)+KLMVN(N2.v, N2.M, N1.v, N1.M);
117 }
118
119
120 public static double KLMVN(Matrix m1, Matrix S1, Matrix m2, Matrix S2)
121 {
122     int d=S1.getColumnDimension();
123     Matrix Deltam=m1.minus(m2);
124
125     return 0.5*(
126         ((S2.inverse()).times(S1)).trace()-d+
127         ((Deltam.transpose()).times(S2.inverse()).times(Deltam)).trace()+
128         Math.log(S2.det()/S1.det())
129     );
130 }
131
132 // scale the trace metric by 1/2
133 public static double ScaledRiemannianSPDDistance(Matrix P, Matrix Q)
134 {
135     double result=0.0d;
136     Matrix M=P.inverse().times(Q);
137     EigenvalueDecomposition evd=M.eig();
138     Matrix D=evd.getD();
139
140     for (int i=0; i<D.getColumnDimension(); i++)
141     {
142         result+=sqr(Math.log(D.get(i, i)));

```

```

143     }
144
145     return Math.sqrt(result/2.0); // ok beta=1/2
146 }
147
148
149
150 public static vM KobayashiMVNGeodesic(vM N0, vM N1, double t)
151 {
152     vM result;
153     Matrix G0, G1, Gt;
154
155     G0=EmbedBlockCholesky(N0);
156     G1=EmbedBlockCholesky(N1);
157
158     Gt=RiemannianGeodesic(G0, G1, t); // Rie geodesic in SPD(2d+1)
159     // Extract
160     result=L2MVN(Gt);
161
162     return result;
163 }
164
165 Matrix RiemannianGeodesic(Matrix P0, Matrix P1)
166 {
167     return RiemannianGeodesic(P0, P1, 0.5);
168 }
169
170
171 public static Matrix RiemannianGeodesic(Matrix P, Matrix Q, double lambda)
172 {
173     if (lambda==0.0) return P;
174     if (lambda==1.0) return Q;
175
176     Matrix result;
177     Matrix Phalf=power(P, 0.5);
178     Matrix Phalfinv=power(P, -0.5);
179
180     result=Phalfinv.times(Q).times(Phalfinv);
181     result=power(result, lambda);
182
183
184     result=(Phalf.times(result)).times(Phalf);
185
186
187
188     return result;
189 }
190
191
192 // Non-integer power of a matrix
193 public static Matrix power(Matrix M, double p)
194 {
195     EigenvalueDecomposition evd=M.eig();
196     Matrix D=evd.getD();
197     // power on the positive eigen values
198     for (int i=0; i<D.getColumnDimension(); i++)

```



```

199         D.set(i, i, Math.pow(D.get(i, i), p));
200
201     Matrix V=evd.getV();
202
203     return V.times(D.times(V.transpose()));
204 }
205
206 public static Matrix EmbedBlockCholesky(vM N)
207 {
208     int i, j, d=N.M.getRowDimension();
209     Matrix Sigma=N.M;
210     Matrix SigmaInv=N.M.inverse();
211     Matrix mut=N.v.transpose();
212     Matrix minusmu=N.v.times(-1.0);
213
214
215     Matrix M, D, L; // Block Cholesky
216     M=new Matrix(2*d+1, 2*d+1);
217     D=new Matrix(2*d+1, 2*d+1);
218
219     D.set(d, d, 1.0);
220
221     // Diagonal matrix
222     for (i=0; i<d; i++)
223         for (j=0; j<d; j++)
224             {
225                 D.set(i, j, SigmaInv.get(i, j));
226                 D.set(d+1+i, d+1+j, Sigma.get(i, j));
227             }
228
229
230
231     M.set(d, d, 1.0);
232
233     for (j=0; j<d; j++)
234     {
235         M.set(d, j, mut.get(0, j)); // row vector
236         M.set(d+1+j, d, minusmu.get(j, 0)); // column vector
237     }
238
239     // add identity matrices
240     for (i=0; i<d; i++)
241         for (j=0; j<d; j++)
242             {
243                 M.set(i, i, 1.0);
244                 M.set(i+d+1, i+d+1, 1.0);
245             }
246
247     // Block Cholesky decomposition
248     L=M.times(D).times(M.transpose());
249
250     return L;
251 }
252
253
254 static vM L2MVN(Matrix L)

```

```

255 {
256     int i, j, d;
257     d= (L.getRowDimension()-1)/2;
258
259     // System.out.println("extract mvn d="+d);
260
261     Matrix Delta=new Matrix(d, d), delta=new Matrix(d, 1);
262     for (i=0; i<d; i++)
263         for (j=0; j<d; j++)
264             {
265                 Delta.set(i, j, L.get(i, j));
266             }
267
268     for (j=0; j<d; j++)
269     {
270         delta.set(j, 0, L.get(d, j));
271     }
272
273     Matrix mu, Sigma;
274
275     // convert natural parameters to ordinary parameterization
276     Sigma=Delta.inverse();
277     mu=Sigma.times(delta);
278
279     return new vM(mu, Sigma);
280 }
281
282
283 public static double FisherRaoMVN(vM N0, vM N1, double eps)
284 {
285     double lb, ub;
286     lb=LowerBoundCalvoOller(N0, N1);
287     ub=UpperBoundSqrtJeffreys(N0, N1);
288     if (ub/lb<1+eps) return ub;
289     else
290     {
291         vM Nmid=KobayashiMVNGeodesic(N0, N1, 0.5);
292         return FisherRaoMVN(N0, Nmid, eps)+FisherRaoMVN(Nmid, N1, eps);
293     }
294 }
295
296     public static double SqrMahalanobisDistance(Matrix m1, Matrix m2, Matrix Sigma
297 )
298 {Matrix res;
299 Matrix m12=m1.minus(m2);
300 res=m12.transpose().times(Sigma.inverse()).times(m12);
301 return res.get(0,0);
302 }
303
304 // non-totally geodesic submanifold
305     public static double FisherRaoSameCovariance(Matrix m1, Matrix m2, Matrix
306 Sigma)
307 {
308 return Math.sqrt(2)*arccosh(1.0+0.25*SqrMahalanobisDistance(m1,m2,Sigma));

```

```

309
310 }
311
312
313 // totally geodesic submanifold
314 public static double FisherRaoSameMean(Matrix m, Matrix S1, Matrix S2)
315 {
316
317 return ScaledRiemannianSPDDistance(S1,S2);
318
319 }
320
321
322
323 public static void main (String [] args)
324 {
325     System.out.println("Fisher-Rao MVN distance");
326     Test();//good
327     //Test2();
328 }
329
330
331 public static Matrix randomSPDCholesky(int d)
332 {
333     int i, j;
334     double [][] array=new double[d][d];
335     Matrix L;
336
337     for (i=0; i<d; i++)
338         for (j=0; j<=i; j++)
339             {
340                 array[i][j]=Math.random();
341             }
342
343     L=new Matrix(array);
344     // Cholesky
345     if (L.det()==0) return randomSPDCholesky(d);
346     return L.times(L.transpose());
347 }
348
349 public static void Test()
350 {
351     Matrix m1, S1, m2, S2;
352     vM N1, N2;
353
354     System.out.println("Test Fisher-Rao distance between multivariate normal
355         distributions");
356
357     m1=new Matrix(2, 1);
358     m1.set(0, 0, 0);
359     m1.set(1, 0, 0);
360     S1=new Matrix(2, 2);
361     S1.set(0, 0, 1.0);
362     S1.set(0, 1, 0);
363     S1.set(1, 0, 0);
364     S1.set(1, 1, 0.1);

```

```

364
365     m2=new Matrix(2, 1);
366     m2.set(0, 0, 1);
367     m2.set(1, 0, 1);
368     //m2=new Matrix(2,1);m2.set(0,0,0);m2.set(1,0,0);
369     S2=new Matrix(2, 2);
370     S2.set(0, 0, 0.1);
371     S2.set(0, 1, 0);
372     S2.set(1, 0, 0);
373     S2.set(1, 1, 1);
374
375     N1=new vM(m1, S1);
376     N2=new vM(m2, S2);
377
378
379
380 double err;
381     double eps=0.01;
382
383     double fr,lb,ub;
384
385     fr=FisherRaoMVN(N1, N2, eps);
386     lb=LowerBoundCalvoOller(N1, N2);
387     ub=UpperBoundSqrtJeffreys(N1, N2);
388     System.out.println("Han & Park 2014 example (mid range).");
389     System.out.println("Fisher-Rao distance (eps="+eps+"):"+fr);
390     System.out.println("lower bound:"+lb+" upper bound:"+ub);
391     // 3.1329
392
393
394
395     m1=new Matrix(2,1);S1=Matrix.identity(2,2);
396     m2=new Matrix(2,1);m2.set(0,0,10000);
397     S2=Matrix.identity(2,2).times(10);
398     N1=new vM(m1, S1);
399     N2=new vM(m2, S2);
400
401     fr=FisherRaoMVN(N1, N2, eps);
402     lb=LowerBoundCalvoOller(N1, N2);
403     ub=UpperBoundSqrtJeffreys(N1, N2);
404     System.out.println("Han & Park 2014 example (long range).");
405     System.out.println("Fisher-Rao distance (eps="+eps+"):"+fr);
406     System.out.println("lower bound:"+lb+" upper bound:"+ub);
407
408     // 23.5
409
410     m1=new Matrix(2,1);m1.set(0,0,Math.random());m1.set(1,0,Math.random());
411     m2=new Matrix(2,1);m2.set(0,0,Math.random());m2.set(1,0,Math.random());
412     S1=S2=randomSPDCholesky(2);
413     N1=new vM(m1, S1);
414     N2=new vM(m2, S2);
415     fr=FisherRaoMVN(N1, N2, eps);
416     double exact;
417     exact=FisherRaoSameCovariance(m1,m2,S1);
418     System.out.println("Same covariance matrix:");
419     System.out.println("Fisher-Rao distance (eps="+eps+"):"+fr);

```

```

420     System.out.println("exact="+exact);
421
422     S1=randomSPDCholesky(2);
423     S2=randomSPDCholesky(2);
424     m1=m2;
425     N1=new vM(m1, S1);
426     N2=new vM(m2, S2);
427     fr=FisherRaoMVN(N1, N2, eps);
428     exact=FisherRaoSameMean(m1,S1,S2);
429     System.out.println("Same mean:");
430     System.out.println("Fisher-Rao distance (eps="+eps+"): "+fr);
431     System.out.println("exact="+exact);
432
433     double sigma1,sigma2;
434     double mu1=Math.random();
435     double mu2=Math.random();
436     m1=new Matrix(1,1);m1.set(0,0,mu1);
437     sigma1=1+Math.random();
438     S1=new Matrix (1,1); S1.set(0,0,sqr(sigma1));
439
440     m2=new Matrix(1,1);m2.set(0,0,mu2);
441     sigma2=1+Math.random();
442     S2=new Matrix (1,1); S2.set(0,0,sqr(sigma2));
443     N1=new vM(m1, S1);
444     N2=new vM(m2, S2);
445     fr=FisherRaoMVN(N1, N2, eps);
446     exact=RaoDistance1D(mu1,sigma1,mu2,sigma2);
447     err=Math.abs(fr-exact)/exact;
448
449     System.out.println("Rao distance in 1d case:");
450     System.out.println("Fisher-Rao distance (eps="+eps+"): "+fr);
451     System.out.println("exact="+exact);
452     System.out.println("relative error="+err);
453 }
454
455     public static void Test2()
456     {int i,nb=200; int d=1;
457     double fr;
458     Matrix m1,S1,m2,S2;
459     vM N1,N2;
460     double eps=0.001;
461
462     for(i=0;i<nb;i++)
463     {
464
465
466     m1=new Matrix(d,1);
467     m2=new Matrix(d,1);
468     for(int j=0;j<d;j++) {m1.set(j,0,Math.random());m2.set(j,0,Math.random());
469     }
470     S1=randomSPDCholesky(d);
471     S2=randomSPDCholesky(d);
472
473
474     N1=new vM(m1, S1);
475     N2=new vM(m2, S2);

```

```
476
477     double jey;
478         fr=FisherRaoMVN(N1, N2, eps);
479     jey=JeffreysMVN(N1,N2);
480     System.out.println(jey+"\t"+fr);
481
482     }
483
484     }
485 }
```